Involvement of host and bacterial factors in Agrobacterium-mediated transformation

Shao, S.

Chapter 2
Analysis of the function of *ADA2* in double strand break repair and *Agrobacterium*-mediated transformation of *Saccharomyces cerevisiae*

Shuai Shao, Daniela M. d'Empaire Altimari, Paul J. J. Hooykaas, G. Paul H. van Heusden

Department of Molecular and Developmental Genetics, Plant Cluster, Institute of Biology, Leiden University, Leiden, 2333 BE, The Netherlands

Abstract

Agrobacterium tumefaciens is the causative agent of crown gall disease and has been extensively used as a vector to create transgenic plants. *Agrobacterium*-mediated transformation (AMT) has become the preferred method for genetic transformation of plants and some fungi and plays critical roles in worldwide agriculture. Under laboratory conditions the yeast *Saccharomyces cerevisiae* can be transformed as well, hence, the mechanism of AMT has been extensively studied using *S. cerevisiae* as model host. Here we report that the absence of *ADA2*, encoding a histone acetyltransferase, results in increased efficiency of AMT by both targeted and random integration. The phenotype of the *ada2Δ* deletion mutant was characterized and we showed that *ADA2* participates in regulation of the cell cycle and DNA damage responses. Overexpression of *SFP1* which is involved in the activation of transcription of ribosomal protein genes, can rescue the methyl methanesulfonate (MMS) sensitivity of the *ada2Δ* deletion mutant. Furthermore, overexpression of *SFP1* attenuates the increased efficiency of AMT of the *ada2Δ* deletion mutant. These results confirm an important role of histone acetylation-deacetylation in AMT. However, more research is needed to elucidate the exact mechanism and to understand the role of *SFP1* in AMT.

Introduction

The soil pathogen *Agrobacterium tumefaciens* is renowned for its ability to transform a broad range of plant species in nature and a lot of non-plant eukaryotic hosts including the yeast *Saccharomyces cerevisiae* under laboratory conditions (Bundock et al., 1995; De Groot et al., 1998). This unique ability of *Agrobacterium* and the high efficiency of *Agrobacterium*-mediated transformation (AMT) made this bacterium essential for plant biology research and made AMT the preferred technology for plant transformations in agricultural industry (for review see: Nester et al., 1984; Gelvin, 2003; Tzfira and Citovsky, 2006; Păcurar et al., 2011; Christie and Gordon, 2014; Gelvin, 2017).

AMT consists of several steps to transfer a DNA segment into the host cell nucleus. This transferred DNA (T-DNA), derived from the *A. tumefaciens* tumor-inducing plasmid (Ti-plasmid), contains genes involved in the synthesis of auxin, cytokinin and opines resulting in uncontrolled cell proliferation and production of opines. Bacterial factors involved in AMT have been characterized in detail (for review see: Christie and Gordon, 2014; Gelvin, 2017). A set of essential proteins encoded by virulence genes (*vir*) present on Ti-plasmids are employed to facilitate this process. Initially, a two-component sensory-response system (VirA/VirG) is triggered to induce the expression of *vir* genes (Winans, 1992). VirD2, together with VirD1, nicks at two 25bp direct repeat border sequences (RB, right border and LB, left border) which flank the T-DNA (Yadav et al., 1982), yielding a single-stranded copy of T-DNA (T-strand) covalently attached to VirD2 at its 5' end (Ward and Barnes, 1988). This complex is transported into the host through a type IV secretion system (T4SS) composed of the VirB1-11/VirD4 proteins (Zhu et al., 2000). Ultimately the T-DNA is integrated into chromosomal DNA via non-homologous recombination (Offringa et al., 1990) by theta-mediated end-joining (TMEJ) with involvement of Polymerase θ (van Kregten et al., 2016). In yeast the T-DNA is preferentially integrated by homologous recombination (HR) (Bundock et al., 1995; van Attikum and Hooykaas, 2003). Alternatively, T-DNA molecules can form complex extrachromosomal structures such as T-circles (Singer et al., 2012; Rolloos et al., 2014) and maintained if possessing a replicator (Bundock et al., 1995). In parallel, several effector proteins (VirE2, VirE3, VirD5 and VirF) are delivered into host cells independently of the T-DNA and contribute to the transformation process (Tzfira et al., 2001; Niu et al., 2015; Schrammeijer et al., 2001; Zhang et al., 2017).

The involvement of host factors in AMT is still not completely understood. Several chromatin components or chromatin-modifying enzymes were identified which play a role in T-DNA integration in plants, such as histone H2A (Mysore et al., 2000) and H3 (Anand et al., 2007) and the histone deacetylases HDT1 and HDT2 (Crane and Gelvin, 2007). The yeast *S. cerevisiae* has been used as an excellent model host to investigate the role of host factors during AMT. More and more host factors involved in AMT have been uncovered by using the yeast complete non-essential gene deletion mutant collections. Histone acetyltransferases (Gcn5, Ngg1, Yaf9 and Eaf7) and deacetylases (Hst4, Hda2 and Hda3) involved in chromatin modification, were identified as factors affecting AMT (Soltani et al., 2009). *ARP6* encoding an actin-related protein that is part of the SWR1 chromatin remodeling complex, negatively regulates AMT (Luo et al., 2015). The cell wall synthesis regulator Smi1 and membrane sterol synthesis scaffold protein Erg28 are also important for efficient AMT (Ohmine et al., 2016). In addition, some proteins can not only affect the efficiency of AMT but also play important roles

in the maintenance of extrachromosomal T-DNA structures. It has been reported that *RAD52*, *RAD51* and *SRS2* are involved in the formation of T-circles in yeast and are necessary for their maintenance (Rolloos et al., 2014; Ohmine et al., 2016).

The Ada2 protein is the chromatin-binding subunit of the SAGA (Spt–Ada–Gcn5 acetyltransferase) histone acetyltransferase complex. This complex is involved in the post-translational modifications of histones that are crucial for chromatin-dependent functions and the regulation of numerous cellular processes in response to environmental cues (Sterner et al., 2002). Ada2 can interact with Gcn5 directly to increase its histone acetyltransferase (HAT) activity which preferentially acetylates histone H3 and histone H2B (Grant et al., 1997; Hoke et al., 2008). Ada2 is evolutionarily conserved among eukaryotes and has been described in several organisms, including *Arabidopsis* (Hark et al, 2009) and *Drosophila* (Muratoglu et al., 2003). In *Arabidopsis*, the orthologs of Ada2 physically associate with Gcn5 and enhance its HAT activity to regulate gene expression under environmental stress conditions such as cold, drought and salt stress (Hark et al, 2009). In 2009, an additional function of Ada2, independent of Gcn5, was identified in yeast. The novel role of Ada2 was to promote transcriptional silencing at telomeres through binding to Sir2 and to prevent the inward spread of heterochromatin regions (Jacobson and Pillus, 2009).

Previous results in our group demonstrated that the deletion of *ADA2* can increase AMT efficiency (Soltani, 2009). In this chapter, we studied the role of *ADA2* in AMT in more detail. To this end, we further characterized the phenotype of the *ada2Δ* deletion mutant and searched for extragenic suppressors of the *ada2Δ* deletion and showed that overexpression of *SFP1*, encoding a transcriptional regulator, suppressed the increased AMT efficiency of *ada2Δ* deletion mutants.

Methods

Agrobacterium strains and growth conditions

Agrobacterium tumefaciens strain LBA1100, a Ti-plasmid-cured derivative of strain C58 containing a *vir* helper plasmid, was used in this chapter (Beijersbergen et al., 1992). All the binary vector plasmids were introduced into *Agrobacterium* by electroporation (den Dulk-Ras and Hooykaas, 1995). *A. tumefaciens* strains were grown and maintained at 29°C in LC medium (10 g/L tryptone, 5 g/L yeast extract and 8 g/L NaCl) containing appropriate antibiotics carbenicillin (100 μg/mL), kanamycin (100 μg/mL) or rifampicin (20 μg/mL) when required.

Yeast strains and growth conditions

S. cerevisiae strains used in this study can be found in Table 1. The deletion mutants were constructed using the PCR-mediated one-step gene disruption method (Baudin et al., 1993). All disruption cassettes and selective markers were amplified from the plasmids listed in Table 2 and the primers used are in Table 3. For labeling of *RAD52*, plasmid pYM27 was used to provide PCR templates for C-terminal EGFP tagging and the primers Rad52-gfp-Fw/Rev were used. For disruption of *ADA2* with the HphMX4 cassette, plasmid pAG32 and primers Ada2-Fw/Rev were used. The PCR products and plasmids were transferred to yeast cells using the lithium-acetate transformation protocol (Gietz et al., 1995). Yeast was grown at 30°C in yeast extract-peptone-dextrose (YPD) medium supplemented, when required, with the appropriate antibiotic G418 (200 μg/mL) or hygromycin (200 μg/mL) or in selective minimal yeast (MY)

medium supplemented with appropriate nutrients. 5-fluoroanthranilic acid (FAA, 500 μg/mL) and 5-fluoroorotic acid (FOA, 500 μg/mL) were used for the counter-selection of tryptophan autotrophs and uracil autotrophs, respectively.

For spot plate assays cultures were adjusted to an OD_{620} of 0.1 after growth to saturation in liquid YPD or MY medium supplemented with appropriate nutrients. Then, ten-fold serial dilutions were made and aliquots of 5 μl were spotted. Dilution assays were incubated at 30°C, except where noted. HU sensitivity was analyzed with serial dilutions from 5 mg/ml. MMS sensitivity was analyzed with serial dilutions from 0.005% to 0.02% MMS and eventually 0.012% MMS was used to screen for genes which can rescue the lethality of *ada2Δ* deletion mutants.

Plasmid construction

The plasmids used in this chapter are listed in Table 2 and the primers are presented in Table 3. To visualize T-DNA via homologous recombination, initially *TRP1* flanking sequences (575 bp sequence at 5'end and 482 bp sequence at 3'end) were amplified from yeast genomic DNA using primers Trp1-up-Fw/Rev and Trp1-down-Fw/Rev and cloned into the *Sac*I/*Bam*HI and *Pst*I/*Hind*III sites, respectively, of the *Agrobacterium* binary vector pCAMBIA2300 to generate the binary vector pCAMBIA2300[*trp1*]. Subsequently, the *lacO* repeats were introduced into T-DNA by cloning the *Bam*HI-*Sal*I fragment with the tandem array of 256 copies of the Lac operator from pAFS59 into vector pCAMBIA2300[*trp1*] to yield pCAMBIA2300[*trp1-lacO*]. Similarly, the *Bam*HI-*Sal*I *lacO* repeats was cloned into vector pCAMBIA2300 to generate pCAMBIA2300[*lacO*]. The test vector pRS425[*lacO*] was constructed by cloning the tandem array of *lacO* repeats digested with *Xho*I and *Sal*I restriction enzymes from pAFS59 into the *Sal*I site of pRS425. All plasmids containing *lacO* repeats were propagated in the *E.coli* STBL2 strain.

To express GFP-Lac repressor fusions in yeast, the segment containing GFP-LacI-NLS (nuclear localization signal) was amplified from the plasmid pAFS152 by PCR using primers LacI-Fw/Rev and cloned into pRS305 digested with *Spe*I and *Sal*I restriction enzymes yielding pRS305-LacI-GFP. Subsequently, the plasmid was linearized by *Nhe*I digestion and integrated into the *LEU2* locus of yeast strain BY4741. To distinguish integrated and extrachromosomal T-DNA, the tandem array of *lacO* repeats were cloned into pSDM8001 between the *PDA1* downstream flank and the right border as well. The tandem array of *lacO* repeats was digested with *Xho*I and *Sal*I restriction enzymes from pAFS59 and then cloned into *Xho*I site of pSDM8001 to generate pSDM8001-*lacO*.

In order to investigate the AMT efficiency of *ada2Δ* deletion mutant, a T-DNA containing *TRP1* flanking sequences was constructed. In brief, the *Xho*I/*Xba*I fragment containing the KanMX marker cassette was digested from plasmid pUG6 and then inserted between the *TRP1* flanking sequences with *Sal*I/*Xba*I sites of pCAMBIA2300[*trp1*] resulting in plasmid pCAMBIA2300[*trp1*-kanMX]. Once T-DNA is integrated into the *TRP1* locus by a double crossover, the *TRP1* will be disrupted and the transformants can be selected on the FAA plates.

Isolation of multi-copy suppressors

The *ada2Δ* strain was transformed with a yeast genomic DNA library in the multi-copy plasmid YEp24 (Carlson and Botstein, 1982) using the standard LiAc method with a few modifications for improving transformation efficiency, such as extending incubation time to 30 or 40 minutes at 42°C. A total of 8,000 transformants were selected on selective minimal medium lacking

uracil (MY-Ura) plates after incubation at 30°C for 2-3 days and then replica-plated onto MY-Ura plates with or without 0.012% MMS. The screen was repeated three independent times. After that, all colonies that grew on both plates were restreaked and candidates were retested at least twice. Subsequently, plasmids were isolated from the remaining 33 transformants using a Plasmid DNA Miniprep Kit (Thermo Fisher Scientific) with addition of lyticase to the resuspension buffer to disrupt cell walls. Then plasmids were propagated in *E. coli* DH10B, isolated and sequenced using general primers YEp24-Fw/Rev from the flanking sequences of the *BamH*I site. The corresponding genomic regions were identified by alignment with the *S. cerevisiae* genome DNA sequence (SGD, www.yeastgenome.org). Each candidate gene was amplified from genomic DNA of BY4741 by PCR using a set of primers 500 bp upstream and 500 bp downstream of the target ORF (Table 3) and the PCR products were cloned in YEp24. The constructed plasmids as well as the parental plasmid YEp24 were introduced into the *ada2Δ* deletion mutant and wild type, respectively, to test the sensitivity towards MMS as described above.

Agrobacterium mediated transformation efficiency test

AMT efficiency was determined as described by Bundock et al. (1995) with some modifications. Firstly, *S. cerevisiae* strains and *Agrobacterium* were cultured overnight at 30°C and 28°C, respectively, under continuous agitation and with the appropriate nutrition or antibiotic selection. The following day, the *Agrobacterium* cells were washed and re-suspended to an OD_{600} of 0.25 in induction medium (IM) with added glucose (10 mM), acetosyringone (AS, 0.2 mM) and the appropriate antibiotics, and incubated for another 6 hours at 28°C. Meanwhile, yeast cultures were diluted to an OD_{620} of 0.1 and incubated in either liquid YPD or MY (when the yeast contains a plasmid) medium. After 6 hours the yeast cells were washed and re-suspended in 0.5 ml of IM, to a final OD_{620} of 0.4 - 0.6 and mixed with an equal volume of *Agrobacterium* cells and vigorously vortexed. Subsequently, 100 µl of the mixture were pipetted onto sterile nitrocellulose filters laid on IM plates supplemented with histidine, leucine and methionine. Once filters were dry, plates were incubated at 21 °C for 6-7 days. After co-cultivation, the cells on each filter were resuspended and then spread onto solid medium containing cefotaxime (200 µg/mL) with or without G418 (200 µg/ml). Finally, after a 3-day incubation at 30 °C, colonies were counted. Yeast AMT efficiency was calculated by dividing the number of colonies on the selective plate by the number of colonies on the non-selective plates. For GFP signal visualization, yeast cells were co-cultivated 2-3 days with *Agrobacterium* cells following the AMT protocol as mentioned above, then washed and re-suspended in MilliQ water or MY medium.

Determination of growth rates

Growth curves were generated by growing cells overnight in MY at 30°C and then diluting them to an OD_{620} of around 0.1. The new cultures were grown at 30°C and the OD_{620} was measured at the indicated time points. All measurements were repeated at least three times in independent experiments.

Assay for cell cycle arrest

The cells used are derivatives of W303a carrying a deletion of the α-factor-inactivating protease, *BAR1*, rendering cells hypersensitive to pheromone and allowing for prolonged cell cycle arrest.

The *ada2*Δ deletion mutant in this genetic background was constructed as described above. The cells were diluted at 0.1 OD_{620} after culturing overnight. The α-factor (Sigma-Aldrich) was added at 1 μg/ml and yeast cells incubated with shaking at 30°C for 3 hrs. Then microscopy was used to check whether more than 90% of the cells were arrested at G1/S phase. To release cells from α-factor arrest, cells were spun down, washed four times and then re-suspended in fresh medium. Cells were collected every half an hour and analyzed by microscopy.

Confocal microscopy

For microscopy a Zeiss Imager M1 confocal microscope equipped with a LSM5 Exciter with a 63x oil objective was used. GFP was detected using an argon laser of 488 nm and a band-pass emission filter of 505-600 nm. Images were processed with ImageJ (ImageJ National Institute of Health) (Schindelin et al., 2012).

Statistical analysis

All data shown are representative of at least three independent experiments of which each contains at least three biological replicates and represented as mean of the performed experiments with standard deviation. Statistic test were done with two-tailed Student's t-test. Statistical analyses were performed using a function equipped in Microsoft Excel. An asterisk indicates the significant differences with the p-values <0.05.

Results

Increased *Agrobacterium*-mediated transformation efficiency of the yeast *ada2Δ* deletion mutant

Before studying the role of *ADA2* in AMT, we compared the transformation efficiency of three different yeast strains, W303a (haploid), BY4741 (haploid) and BY4743 (similar as BY4741, but diploid). To this end, these strains were transformed with the *Agrobacterium* strain LBA1100 carrying pRAL7100 allowing integration of *URA3* into the *PDA1* locus by homologous recombination (Figure 1A) (Bundock et al., 1995). As illustrated in Table S1A, the transformation efficiency of the diploid strain BY4743 is highest ($1.2 \pm 0.2 \times 10^{-4}$ n=3) and the haploid strain BY4741 has a higher transformation efficiency than the haploid strain W303a at frequencies of $9.7 \pm 0.3 \times 10^{-5}$(n=3) and $1.4 \pm 0.04 \times 10^{-5}$ (n=3), respectively. Compared to the frequencies of W303a, it was 6.9-times higher in BY4741 and 8.6-times higher in BY4743. Therefore, and because of the high level of auto-fluorescence of W303a cells, we used strain BY4741 and derived mutants for our further research. In addition, we prefer a haploid strain over a diploid strain because genetic manipulations are easier in haploid strains.

Previously we showed that the *ada2Δ* deletion mutant in the diploid BY4743 background has an increased transformation efficiency (Soltani et al., 2009). To investigate whether this is also the case in the haploid BY4741 background, we constructed an *ada2Δ* deletion mutant in BY4741 by replacing the coding sequences by an hygromycin resistance marker. As shown in Figure 1C and Table S1B, an *ada2Δ* deletion mutant in the haploid BY4741 background has a 4-fold increased transformation efficiency compared to the parental strain at frequencies of $1.1 \pm 0.6 \times 10^{-4}$ and $4.4 \pm 0.8 \times 10^{-4}$, respectively. The effect of the *ada2Δ* deletion on T-DNA integration may be different for different chromosomal loci. To further investigate this possibility, we constructed a new binary vector containing T-DNA in which the

KAN.MX marker is flanked by sequences allowing integration by homologous recombination into the *TRP1* locus instead of into the *PDA1* locus (Figure 1B). The *TRP1* locus is physically close to the centromere on chromosome IV, whereas the *PDA1* locus is located at the end of chromosome V. When using *TRP1* as target, also counter-selection is possible allowing screening of transformants for loss of the *TRP1* gene due to the integration of the T-DNA (Toyn et al., 2000). Therefore, after co-cultivation, the yeast cells were forward-selected using the KAN.MX marker. Subsequently, transformants were replicated to plates supplemented with or without 5-fluoroanthranilic acid (FAA), which is used for the counterselection of *TRP1*. Using this T-DNA the transformation frequency of the *ada2Δ* strain was around 2-fold higher than that of the BY4741 strain ($1.2\pm 0.7 \times 10^{-4}$ vs $0.6 \pm 0.3 \times 10^{-4}$) (Figure 1D, Table S1B). In the wild type strain, only few transformants (2.4 ± 0.5 %) could not survive on the plates supplemented with FAA suggesting that in most transformants the T-DNA was integrated into the *TRP1* locus disrupting the synthesis of tryptophan (Table S1C). In the *ada2Δ* background, around one third of transformants (27 ± 5 %) were not able to grow on plates containing FAA, indicating that in *ada2Δ* in a large number of the transformants the *TRP1* locus is still intact. This was confirmed by PCR for 7 of these colonies that were randomly chosen. This suggests that in the *ada2Δ* background AMT gives much more transformants (>10 fold) in which the T-DNA has not integrated at the *TRP1* locus in the chromosomal DNA.

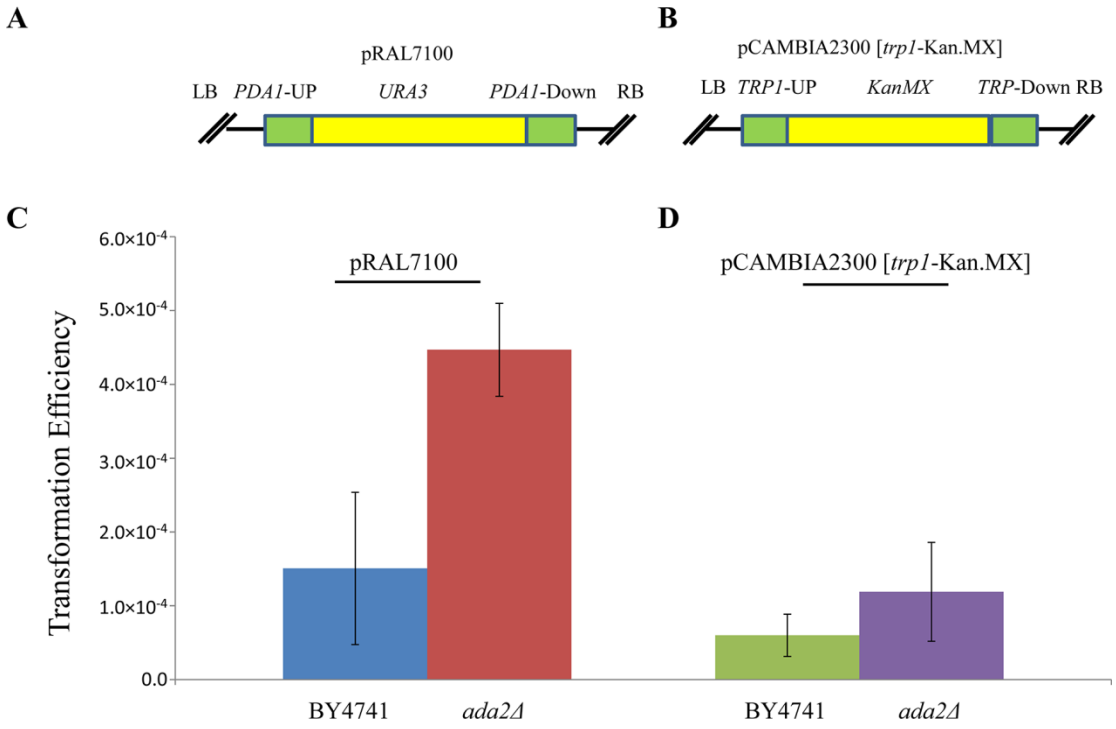

Figure 1. Increased *Agrobacterium*-mediated transformation efficiency of the yeast *ada2Δ* deletion mutant by HR. Yeast strain BY4741*ada2Δ* and its parent strain BY4741 were co-cultivated with *Agrobacterium* strain LBA1100 harboring pRAL7100 or pCAMBIA2300[*trp1*-kanMx]. The schematic diagrams present the structure of the T-DNA of pRAL7100 (A) and of pCAMBIA2300[*trp1*-kanMx] (B). AMT efficiency for *Agrobacterium* strains carrying pRAL7100 and pCAMBIA2300[*trp1*-kanMx] are shown in panels C and D, respectively. Error bars indicate the standard deviations of triplicate independent assays.

Foreign DNA can be introduced into yeast cells by other methods which don't employ *Agrobacterium* such as LiAc transformation or electroporation. In a number of experiments we transformed BY4741 and the *ada2Δ* deletion mutant with linear DNA fragments like constructs allowing integration of GFP at the *RAD52* locus or with plasmids like the overexpression plasmid YEp24 using the LiAc transformation protocol. Although we did not study the effect of deletion of *ADA2* on the efficiency of the LiAc transformation in a systematic way, we observed a decreased rather than an increased transformation efficiency for the *ada2Δ* deletion mutant. In a transformation experiment aimed to tag *RAD52* with GFP (see below), around one hundred transformants were obtained for the wild type strain BY4741, whereas less than 20 transformants were obtained for the *ada2Δ* deletion mutant. The number of transformants of the *ada2Δ* deletion mutant after transformation with plasmid YEp24 was much lower than the number of transformants of BY4741 (approx. 20 *vs* approx. 100). Thus, the increased transformation efficiency of *ada2Δ* deletion mutant is specific for AMT in accordance with previous results from our group (Soltani, 2009)

Integration of T-DNA by NHEJ

Although homologous recombination is the predominant mechanism of T-DNA integration in yeast, integration via non-homologous end-joining is possible as well (Bundock and Hooykaas, 1996; van Attikum et al, 2001). In order to investigate the effect of the *ada2Δ* deletion on T-DNA integration via NHEJ, we exploited *Agrobacterium* strain LBA1100 harboring plasmid pRAL7102. This plasmid contains T-DNA with the *URA3* marker but has almost no homology with the BY4741 genome (see below) and no yeast replication origin (Figure 2A). As illustrated in Figure 2A, *Agrobacterium* carrying pRAL7102 is able to transform BY4741, but at an extremely low frequency of $2.4 \pm 1.4 \times 10^{-6}$. Compared with the wild type strain, the transformation efficiency ($1.0 \pm 0.2 \times 10^{-4}$) was much higher for the *ada2Δ* deletion mutant, indicating that also AMT via NHEJ is affected by the *ADA2* deletion. To prevent homology between T-DNA and recipient's genome, we used BY4741 derived strains as recipients in which the *URA3* locus had been removed completely (Figure 2B). However, a short sequence of 47 bp was found on T-DNA close to the RB that has homology to a region of yeast chromosome V adjacent to *URA3*. This may imply a small chance for T-DNA integration by HR through a single cross-over rather than a double cross-over. To investigate integration into the *URA3* locus, we analyzed the *URA3* locus in five randomly selected transformants by PCR. Using primer pair URA3-C / URA3-D a fragment of 150 bp is expected when the T-DNA is not integrated into the *URA3* locus, whereas a larger fragment is expected when the T-DNA is integrated at this locus (Figure 2C, left part). For all of the selected transformants, the expected 150 bp fragment was obtained, indicating that the chromosomal *URA3* locus was not altered, excluding integration of the T-DNA at the *URA3* locus. On the other hand, using primer combination URA3-A / URA3-B which has no homology to the BY4741 genome, but can amplify the *URA3* originating from the T-DNA, a band of 565 bp was found for all five transformants indicating the presence of the T-DNA (Figure 2C, right part).

In order to further investigate whether the T-DNA was integrated into one of the chromosomes or whether it was present as extrachromosomal structures, some of the transformants were streaked on plates containing 5-fluoro-orotic acid (5-FOA). It is expected that transformants with the T-DNA integrated into one of the chromosomes will not be able to

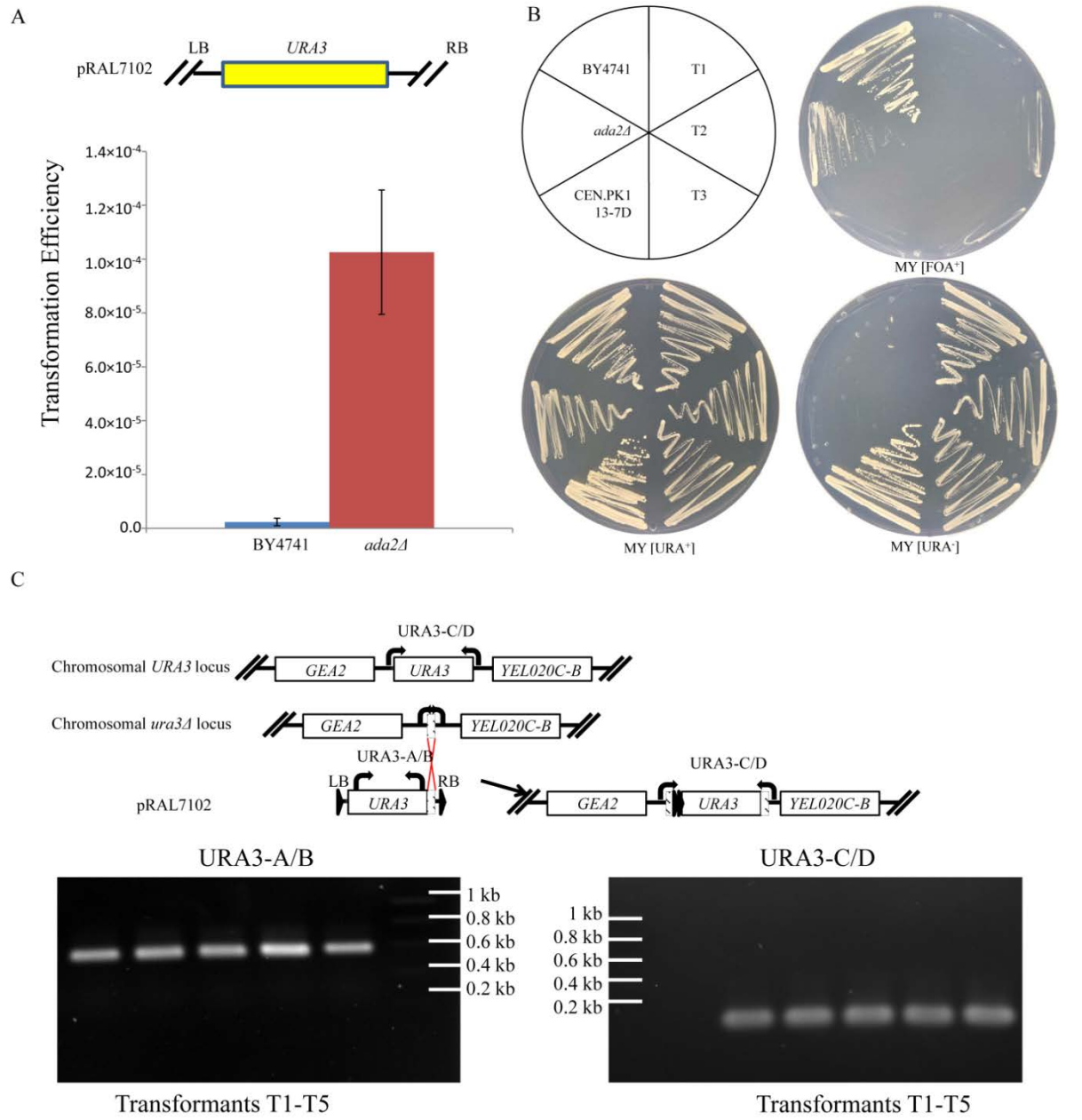

Figure 2. Increased *Agrobacterium*-mediated transformation efficiency of the yeast *ada2Δ* deletion mutant by NHEJ. Yeast strain BY4741*ada2Δ* and its parent strain BY4741 were co-cultivated with *Agrobacterium* strain LBA1100 harboring pRAL7102. (A) The structure of the T-DNA used and the effect of the *ADA2* deletion on AMT efficiency via NHEJ. Error bars indicate the standard deviations of triplicate assays. (B) The transformants generated by non-homologous T-DNA were used for further study. Growth on plates either with 5-FOA or without 5-FOA was used to detect whether the *URA3* marker was stably integrated in the genome or could be lost. The wildtype BY4741, CEN.PK113-7D and *ada2Δ* deletion mutant were included as controls. (C) The presence of the selective *URA3* marker was determined with the primer pair URA3-A/B via PCR. Due to the short homologous sequence of 47 bp found in T-DNA mentioned above, T-DNA may integrate at the *URA3* locus by HR through a single cross-over. The primer pair URA3-C/D was used to check for integration at the *URA3* locus. All DNA templates were isolated from individual transformants.

grow in the presence of 5-FOA, whereas transformants with the T-DNA on extrachromosomal structures are able to grow slowly on media with 5-FOA as extrachromosal DNA structures are usually unstable on non-selective media. In total, 16 transformants of BY4741 and 104 transformants of the *ada2Δ* deletion mutant from three independent experiments were analyzed. All analyzed transformants were able to grow on plates lacking uracil, but not on plates with 5-FOA indicating that the *URA3* selection marker of the T-DNA was stably maintained and expressed. Further growth analysis showed that one of six tested transformants of BY4741 did grow slowly on 5-FOA, but none of the eighteen selected transformants of the *ada2Δ* deletion mutant were able to grow in the presence of 5-FOA, indicating that these transformants cannot easily loose the T-DNA. The effect of 5-FOA on three selected representative transformants and on an uracil prototrophic (CEN.PK113-7D) and auxotrophic (BY4741) control strain is shown in Figure 2B.

The *ada2Δ* deletion mutant has a slow growth phenotype

It has been reported that *ada2* mutants have a decreased growth compared to the corresponding parental strains (Berger et al., 1992). As the increased transformation efficiency of the *ada2Δ* mutant may be related to the decreased growth rate of this mutant we compared the growth of the *ada2Δ* deletion mutant in BY4741 with that of the parental strain. As illustrated in Figure 3A, the *ada2Δ* deletion mutant indeed grew slower than BY4741 (growth rates: 0.184 ± 0.007 h^{-1} and 0.150 ± 0.011 h^{-1}; n= 4, P=0.0019 for *ada2Δ* and BY4741, respectively). Also the *ada2Δ* deletion mutant formed slightly smaller colonies than the BY4741 strain, both on rich (YPD) and minimal (MY) medium (Figure 3B). In another experiment we showed that also the *ada2Δ* deletion mutant harboring plasmid YEp24 grows significantly (P=0.048) slower than BY4741 carrying this plasmid (0.176 ± 0.027 h^{-1} *vs* 0.247 ± 0.034 h^{-1}, respectively) (see also Figure 8).

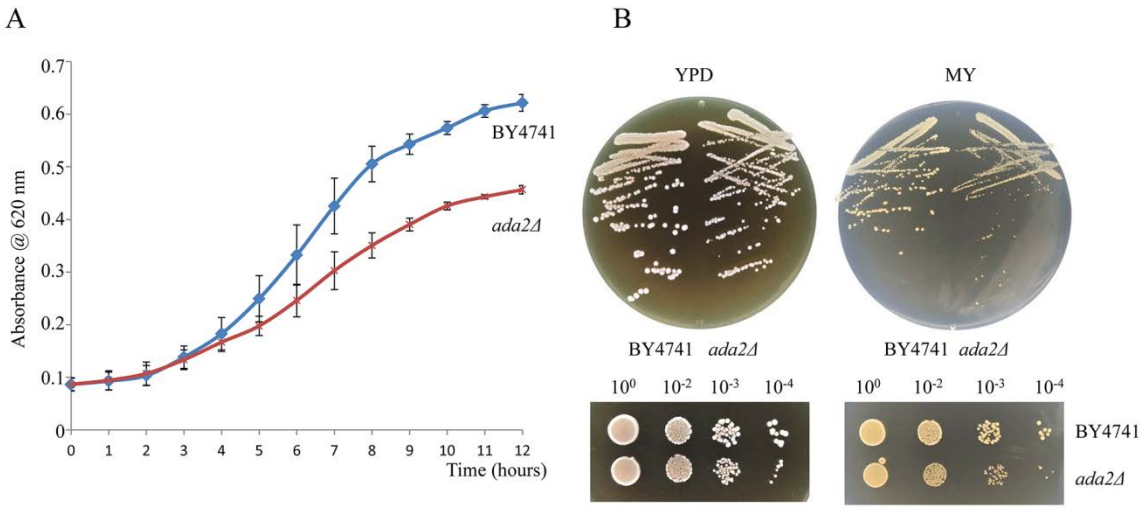

Figure 3. The *ada2Δ* deletion mutant grows more slowly than the wild type BY4741. (A) Analysis of the effect of the *ADA2* deletion on growth in liquid culture. Dilutions of yeast cells were inoculated into MY media after overnight culture in rich medium YPD and absorbance measurements were performed at the indicated time points. Error bars indicate the standard deviations of three independent replicates. (B) Analysis of the effect of the *ADA2* deletion on growth on plates. Both wild type BY4741 and *ada2Δ*

deletion mutant were tested on rich YPD and minimal MY plates. Yeast cells were serially diluted and spotted onto the plates. The photos were taken after three days and the experiment was performed three independent times. Results of representative plates are shown.

A

Cell morphology	BY4741 (%)		*ada2Δ* (%)	
Non-budded	38/138 (27.5%)	60/171 (35.1%)	9/62 (14.5%)	14/81 (17.3%)
Budded	100/138 (72.5%)	111/171 (64.9%)	53/62 (85.5%)	67/81 (82.7%)

B

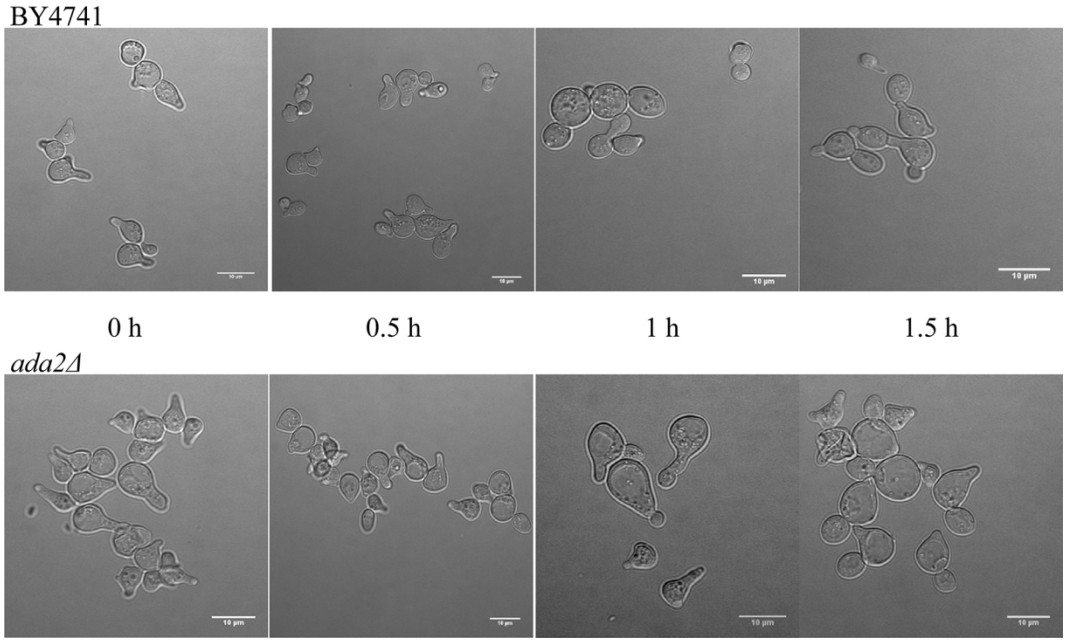

Figure 4. The effect of the *ada2Δ* deletion on cell cycle progression. (A) Analysis of budding by microscopy. Yeast cells were cultured in minimal liguid medium until log phase. Then the images of cell populations were taken and the numbers of budding and non-budding yeast cells were manually counted. (B) Analysis of cell cycle progression after release from α-factor arrest. α-factor was used to arrest wild type and *ada2Δ* deletion mutant cells at G1/S phase. Cells were collected at the indicated times after release from α-factor arrest. The wildtype W303 *bar1Δ* recovered rapidly and continued to grow (upper panel). However, the *ada2Δ* deletion mutant presented significant growth deficiency (lower panel).

It is well known that Ada2 is a general transcriptional regulator and the expression of 2.5% of the genes is affected at least 2-fold by the *ADA2* deletion (Hoke et al., 2008). Combined with the lower growth of its deletion mutant, it is conceivable that some genes regulated by Ada2 can affect the cell cycle of yeast cells. To get more insight in the effect of the *ADA2* deletion on the cell cycle, the number of budded cells present in exponentially growing cultures of BY4741 and *ada2Δ* cells were counted. As shown in Figure 4A, 72.5% / 64.9% of the BY4741 cells and 85.5% / 82.7% of the *ada2Δ* cells were budded, suggesting a slight difference of their cell cycle. To further investigate whether the *ADA2* deletion affected a specific moment in the cell cycle, we made use of the *bar1Δ* deletion mutant in the W303 background allowing arrest at

the G1-S boundary by the α-factor and constructed an *ada2Δ* deletion in this strain. More than ninety percent of both wild type and *ada2Δ* deletion mutant cells have small buds when arrested by the α-factor (Figure 4B). In the first 1.5 hours after release from the α-factor arrest the bud size strongly increased in wild type cells, but not in *ada2Δ* cells (Figure 4). Only after 2 hours the bud size of these cells started to increase. These experiments may indicate that *ada2Δ* cells are delayed in the S-phase of the cell cycle. However, additional experiments have to be performed to show whether or not *ADA2* specifically regulates this phase of the cell cycle.

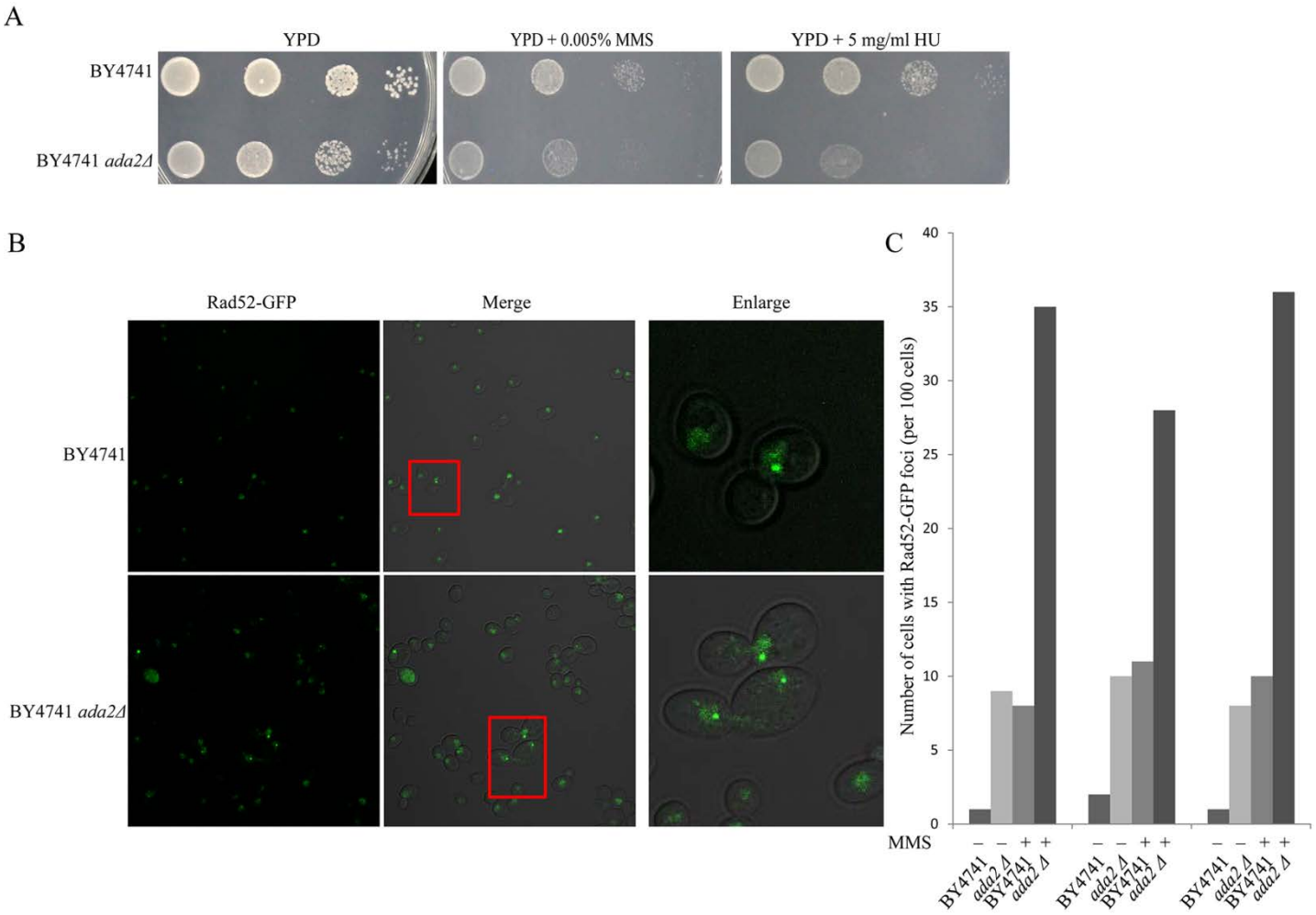

Figure 5. The *ada2Δ* deletion mutant is more sensitive to the DNA damaging agents MMS and HU and has an increased number of double strand breaks. (A) Both wild type BY4741 and *ada2Δ* deletion mutant were tested on YPD plates with two commonly used DNA damaging agents, MMS and HU. Yeast cells were serially diluted and spotted onto the plates. The photos were taken after three days and representative results of three independent experiments are shown. (B) The Rad52 protein was marked by GFP to visualize DSBs in yeast cells. The DNA repair foci were observed using confocal microscopy. (C) The number of DNA repair foci is increased in the *ada2Δ* deletion mutant both with or without the addition of MMS. The data from three independent experiments are shown.

The *ada2Δ* deletion mutant is more sensitive to DNA damaging agents

Ada2-dependent histone acetylation may be involved in double strand break (DSB) repair (Muñoz-Galván et al., 2013). As DSBs may promote AMT we investigated the sensitivity of the *ada2Δ* deletion mutant for DNA damaging agents. The DNA alkylating agent methyl methanesulfonate (MMS) has been used for many years to induce double-stranded breaks during replication and hydroxyurea (HU) is a potent inhibitor of the enzyme ribonucleotide reductase (RNR) in S-phase and leads to stalling of DNA replication. Survival viability was estimated by plating serial dilutions of cultures of wild type and *ada2Δ* deletion mutant cells on YPD plates containing MMS or HU. Then all plates were incubated at 30°C for 2 days. As demonstrated in Figure 5A, the deletion of *ADA2* enhanced the sensitivity to the DNA damaging agents MMS and HU. To obtain more direct evidence for the presence of chromosomal DNA damage accidents in *ada2Δ* mutants, we analyzed *Rad52* foci formation in the absence and presence of MMS. *Rad52* is a master regulator protein of DNA repair via homologous recombination and *Rad52* is recruited at DSBs which can be seen as foci when using GFP-tagged Rad52 (Lisby et al., 2001). Such foci were also formed in the *ada2Δ* deletion mutant (Figure 5B). As shown in Figure 5C, the number of *Rad52* foci in the *ada2Δ* mutant seems higher than that in the wild type. However, upon treatment with MMS, the number of *Rad52* foci is around three fold higher in the *ada2Δ* mutant compared to the wild type strain. In other words, in the *ada2Δ* mutant there is more DNA damage or repair is slower and this could lead to chromosomal DNA instability which may contribute to the integration of T-DNA.

Overexpression of *SFP1* can rescue the MMS sensitivity of the *ada2Δ* deletion mutant

To gain more insight into why yeast cells lacking *ADA2* are hypersensitive to DNA damaging agents, we performed a synthetic rescue screen (Figure 6A). To this end, a YEp24-based *S. cerevisiae* genomic DNA overexpression library (Carlson and Botstein, 1982) was transformed into the *ada2Δ* deletion mutant. First Ura^+ transformants were selected and subsequently all transformants were copied to plates supplemented with MMS to screen for MMS resistant transformants. From approximately 80,000 transformants, 32 of them could grow on MY plates containing 0.01 % MMS. Plasmids, isolated from candidate yeast transformants, were transformed into *E. coli* to be sequenced. Sequence analysis indicated that 6 distinct genetic loci were represented among the original yeast transformants (Figure 6B). Of these 32 candidates, most (23 candidates) contained the *ADA2* gene. To identify which gene on the other plasmids is responsible for the viability of the original transformants, each hypothetical gene was individually inserted into YEp24 and introduced back into the original recipient *ada2Δ* deletion mutant. As a control, the empty vector YEp24 was used. To investigate whether the effects of overexpression of the candidate genes are specific for the *ada2Δ* deletion mutant, also the wild type strain BY4741 was transformed with the empty vector YEp24 or with YEp24 carrying the candidate genes. After selection for resistance to MMS only two candidate genes (*HEM2* and *SFP1*) remained (Figure 6C). However, BY4741 cells carrying YEp24 with *HEM2* were also more resistant to MMS compared to the BY4741 cells carrying the empty YEp24 vector. In contrast, the effect of *SFP1* was specific for the *ada2Δ* deletion mutant (Figure 6C). Cells of the *ada2Δ* deletion mutant carrying YEp24 with *HEM2* or *SFP1* were not more resistant to HU compared to cells carrying the empty vector, indicating that the effects are specific for the

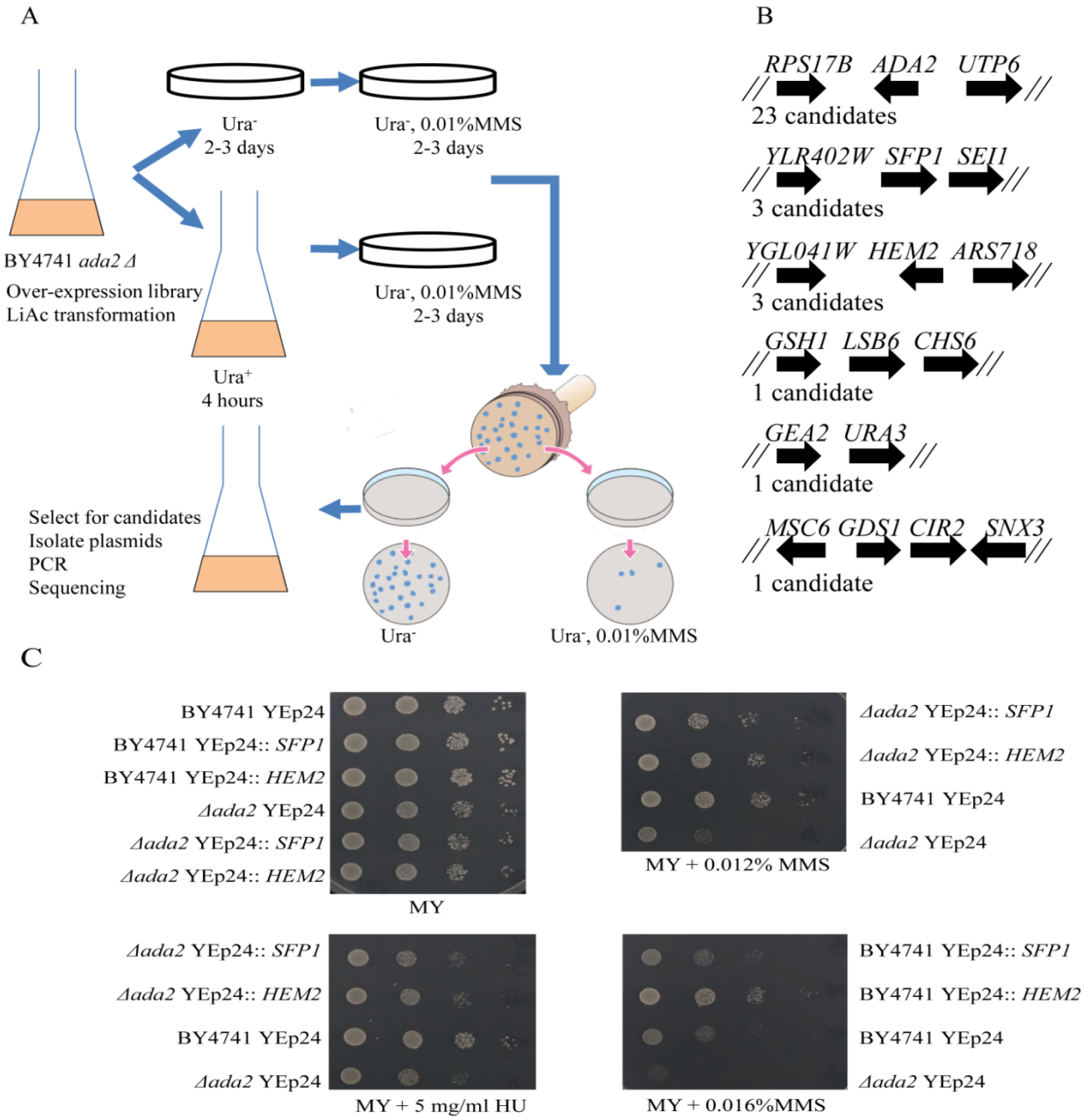

Figure 6. A genome-wide overexpression screen to identify genes that can suppress the MMS sensitivity of the *ada2Δ* deletion mutant. (A) schematic diagram of the synthetic rescue experiment. In brief, the whole genome-wide library was transformed into *ada2Δ* deletion mutant and plated on supplemented MY medium lacking uracil. Subsequently, all transformants were copied and spotted onto supplemented MY medium lacking uracil with MMS to test their sensitivity. (B) schematic representation of the yeast chromosomal regions contained in the YEp24 genomic DNA clones obtained by the synthetic rescue experiments. All candidates were from the combination of three independent experiments. After that, each single candidate including its promoter region was cloned into YEp24 vector and introduced in *ada2Δ* deletion mutant again to test for sensitivity to MMS. (C) MMS resistance in *ada2Δ* deletion mutant can be rescued by overexpression of *SFP1* and *HEM2*. The overexpression vector YEp24 containing *SFP1* or *HEM2* were introduced into *ada2Δ* deletion mutant and wild type BY4741. The empty plasmid YEp24 was introduced as control. All mutants were serially diluted and spotted onto MY medium with appropriate concentrations of MMS. After 3 days, the photos were taken and the spot assays were performed at least three independent times.

sensitivity to MMS. *HEM2* is an essential gene, encoding a homo-octameric enzyme involved in heme biosynthesis and *SFP1* is a non-essential gene which is involved in the activation of transcription of the genes encoding ribosomal proteins (Saccharomyces Genome Database, SGD, www.yeastgenome.org)(Marion et al., 2004). These experiments indicate that there is a genetic interaction between *SFP1* and *ADA2* in the response to the DNA damaging agent MMS.

Overexpression of *SFP1* affects the efficiency of AMT in the *ada2Δ* deletion mutant

To investigate whether overexpression of *SFP1* in the *ada2Δ* deletion mutant can affect AMT efficiency, we co-cultivated the *ada2Δ* deletion mutant and the parental strain BY4741 carrying YEp24[*SFP1*] or the empty vector with *Agrobacterium* strain LBA1100 (pRAL7100). As shown in Figure 7, the increased transformation efficiency of the *ada2Δ* deletion mutant is abolished after introduction of YEp24[*SFP1*]. Such an effect was not seen for the BY4741 control strain.
Both Ada2 and Gcn5 are components not only of the ADA, but also of the SAGA histone acetyltransferase complex (Balasubramanian et al., 2002; Sun et al., 2018). In addition, both of them are required for repair of DNA damage (Mckinney et al., 2013). To determine whether overexpression of *SFP1* also affects the *gcn5Δ* deletion mutant, we generated a *gcn5Δ* deletion mutant and introduced YEp24[*SFP1*] or the empty vector. As shown in Figure 7, there was no significant difference in AMT efficiency between the *gcn5Δ* deletion mutant harboring the overexpression vector with *SFP1* or the empty vector. No effect of the *gcn5Δ* deletion on AMT was found, which is in contrast with previous observations in the diploid BY4743 background (Soltani et al., 2009).

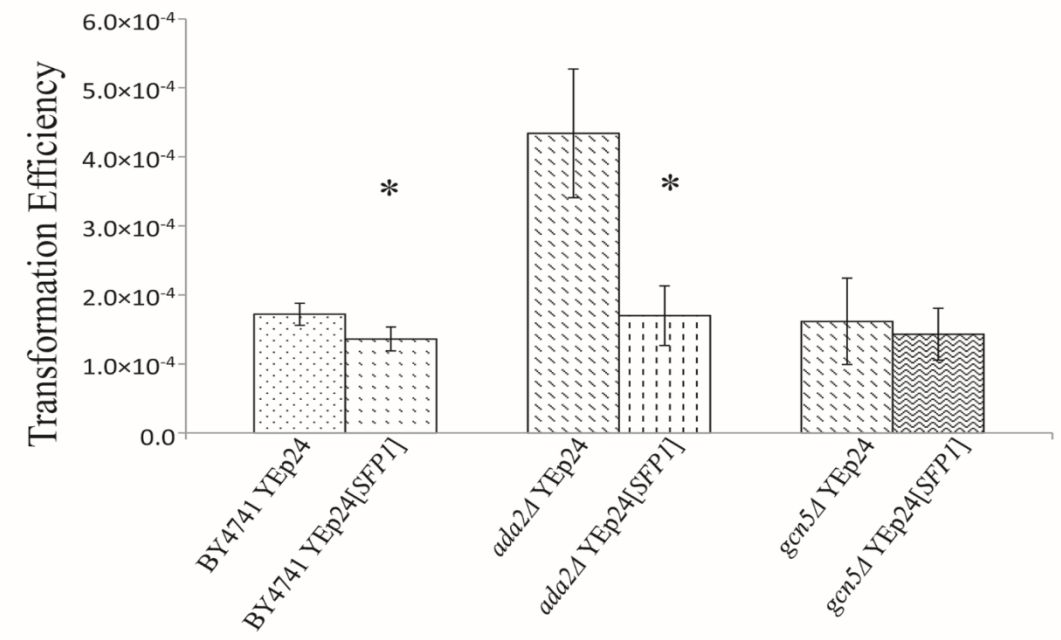

Figure 7. Effect of overexpression of *SFP1* on AMT efficiency. Yeast strains BY4741, BY4741*ada2Δ* and BY4741*gcn5Δ* containing YEp24 or YEp24[SFP1] were co-cultivated with *Agrobacterium* strain LBA1100 harboring pSDM8001 and AMT efficiency was determined. Error bars indicate the standard deviations of triplicate independent assays. Differences were statistically significant comparing overexpression of *SFP1* with its corresponding control by Student's test. *: $P < 0.05$.

The effect of overexpression of *SFP1* on *ada2Δ* is probably not related to the role of *SFP1* in regulation of the TORC1 complex nor to an effect on the growth rate

The proposed dominant cellular role of *SFP1* is regulation of transcription of ribosomal protein and biogenesis genes (Jorgensen et al., 2004). It has been shown that Sfp1 interacts directly with the Target of Rapamycin Complex 1 (TORC1) in a rapamycin-regulated manner, and that Sfp1 is phosphorylated by this kinase complex. On the other hand, Sfp1 negatively regulates TORC1 suggesting feedback mechanisms controlling the activity of these proteins in response to different nutrient and stress conditions (Lempiainen et al., 2009). To investigate a possible role of *ADA2* in the TORC pathway 27 genes involved in the this pathway or involved in regulation of TORC1 signaling were selected (Table S2) and overexpression vectors harboring these genes were obtained from the Yeast Genomic Tiling Collection. These vectors were introduced into the *ada2Δ* deletion mutant and the sensitivity to MMS was tested. After the first screen (supplementary Figure S1A) 10 potential candidates (*MRS6, LST8, LST7, TCO89, SEA4, VAM6, GTR1, GTR2, LST4* and *TOR1*) were further tested. As each vector from this collection contains more than one gene, candidate genes were amplified from yeast genomic DNA, cloned into the multi-copy vector pRS425 and introduced into the *ada2Δ* deletion mutant. As controls, both the vector pRS425 containing *SFP1* and the empty vector were introduced into the wild type strain BY4741. As demonstrated in Figure S1B, unlike *SFP1*, none of these genes on a multi-copy plasmid could rescue the sensitivity towards MMS of the *ada2Δ* deletion mutant. Thus, these observations didn't provide evidence for involvement of the TORC pathway in sensitivity of the *ada2Δ* deletion mutant towards MMS, but did not exclude such a role.

More recently, Ohmine et al. showed that deletion of *ERG28* resulted in a decreased AMT efficiency and that growth of the *erg28Δ* strain was unaffected by the presence of donor bacterial cells, while the growth of the wild type and other mutant yeast strains was suppressed by their presence (Ohmine et al., 2016). This may imply that the growth rate affects AMT efficiency. It has been reported that *SFP1* may also be involved in the regulation of cell division and the cell cycle (Jorgensen et al., 2002; Albert et al., 2019). Hence, we determined the effect of overexpression of *SFP1* on the growth rate of wild type, *ada2Δ*, *gcn5Δ* and *ada2Δgcn5Δ* strains cultured in liquid medium. As shown in Figure 8, the growth rate of the tested deletion mutants was lower compared with that of the wild type strain. However, their growth rates were not restored by overexpression of *SFP1*, suggesting that the effect of overexpression of *SFP1* on AMT efficiency is not related to an effect on the growth rate.

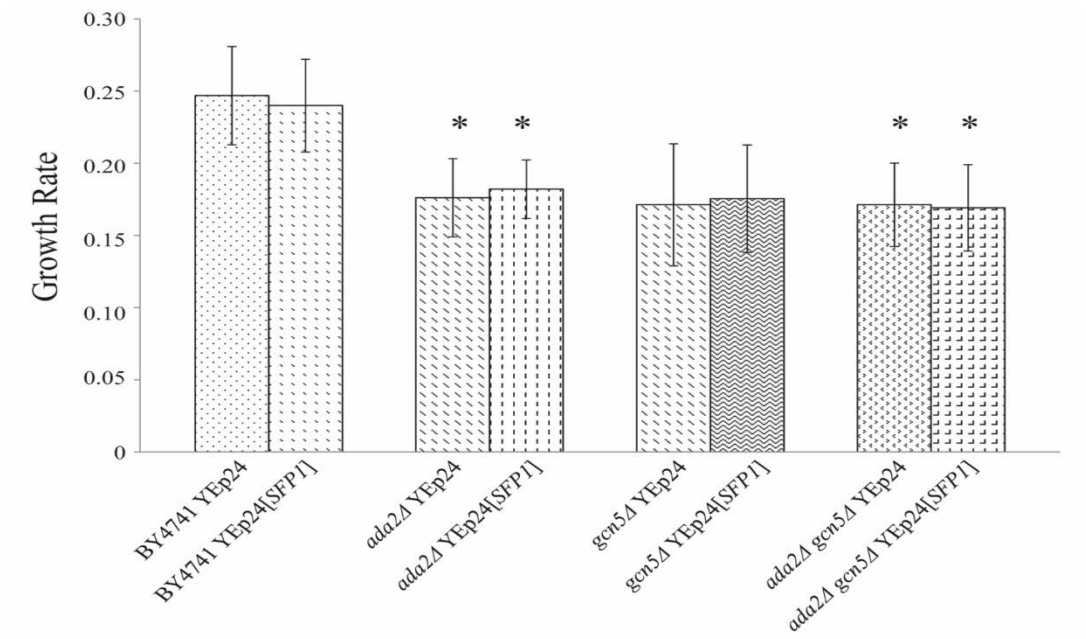

Figure 8. Effect of overexpression of *SFP1* on the growth rates of different yeast strains. The yeast cells were cultured overnight, then diluted to a final OD_{620} of 0.1 and inoculated into fresh medium on the next morning. The OD_{620} was systematically measured every hour until a total of 8 time points. Values were normalized and three growth curves were obtained for each mutant. Analysis of the curves by fitting to an exponential trend line yielded the growth rate. Afterwards, average growth rate for each mutant was calculated together with their SD (Standard deviation). Error bars indicate the standard deviations of triplicate assays and each contains three independent replicates. Differences were statistically significant compared to strain BY4741 YEp24 by Student's test. *: $P < 0.05$.

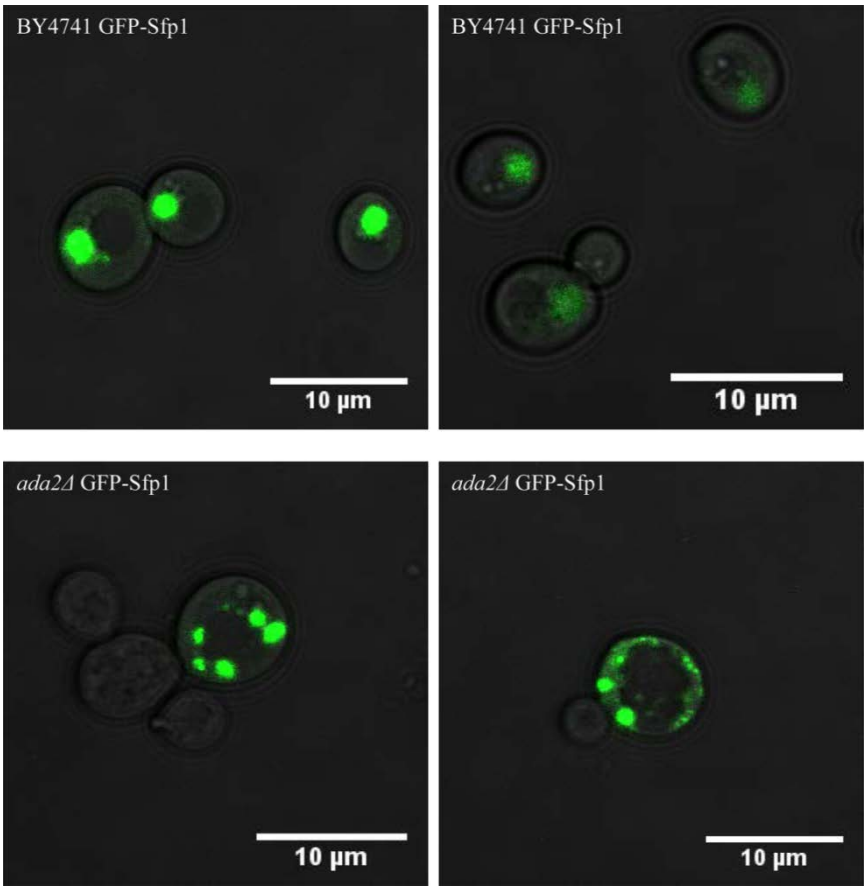

Figure 9. Visualization of the subcellular localization of GFP-Sfp1 in BY4741 and *ada2Δ* deletion mutant cells. BY4741 and BY4741*ada2Δ* were transformed with plasmid pUG34[SFP1] encoding the GFP-Sfp1 fusion protein. Yeast cells were cultured overnight and then analyzed by confocal microscopy. The experiment was repeated three independent times and similar results were obtained.

Sfp1 is regulated, at least in part, by its subcellular localization (Lempiainen et al., 2009). In optimally growing cells, Sfp1 is predominantly nuclear and localizes to a number of Ribosomal Protein gene promoters. By contrast, unfavorable nutrient conditions or stress lead to a rapid re-localization of Sfp1 from the nucleus to the cytoplasm. Therefore, we investigated the effect of the *ada2Δ* deletion on the localization of Sfp1. To this end, we used the centromeric plasmid pUG34 to express a GFP-Sfp1 fusion protein. After 24 hours of culture, GFP-Sfp1 is still concentrated in the nucleus in the wild type strain BY4741, while in the *ada2Δ* deletion mutant most of GFP-Sfp1 was present in multiple unknown structures (Figure 9). This observation suggests that deletion of *ADA2* makes yeast cells more sensitive to environmental stress or to other unfavorable factors. In other words, in the absence of Ada2, Sfp1 failed to localize in the nucleus, indicative of stress caused by persistent DNA damage in the *ada2Δ* deletion mutant.

Visualization of T-DNA in *ada2Δ* and BY4741 cells during co-cultivation with *Agrobacterium*

To compare the fate of the T-DNA translocated from *Agrobacterium* into *ada2Δ* cells with that of T-DNA translocated into BY4741 cells, we attempted to visualize the T-DNA during AMT. To this end a series of *Agrobacterium* binary vectors harboring *lacO* repeats were constructed. The plasmid pCAMBIA2300[*trp1-lacO*] contains an array of 256 *lacO* repeats on its T-DNA flanked with sequences of the yeast *TRP1* locus. Upon translocation of this T-DNA from *Agrobacterium* into yeast cells expressing the Lac repressor tagged with GFP, the T-DNA may become visible (Figure 10A). This system has been used successfully before for example to visualize chromosome duplication (Straight et al., 1996).

To order to test this system, we introduced the 256 tandem *lacO* repeats in the high-copy vector pRS425 and then transferred the plasmid into the yeast strain expressing the fusion protein LacI-GFP. As can be seen in the Figure 10B, there are multiple dots representing the *lacO* array in the nuclei of this strain. Upon co-cultivation of BY4741 or *ada2Δ* expressing LacI-GFP with *Agrobacterium* carrying pCAMBIA2300[*trp1-lacO*] only a few cells containing fluorescent structures could be detected. AMT efficiency of *ada2Δ* was around 1.0×10^{-4} and that of BY4741 was half that; therefore, it is not surprising that the number of cells with fluorescent signal was low even we observed more than 10,000 cells in every independent experiment. As shown in Figure 10C a single fluorescent dot was found in one of the cells of the wild type strain and two dots were found in one of the *ada2Δ* cells expressing LacI-GFP. Unfortunately, only a low number of fluorescent cells were found preventing statistical analysis.

In order to monitor unintegrated T-DNA, a new T-DNA construct was generated with the KanMX selection marker flanked by sequences of the *PDA1* gene and with the 256 tandem repeats of the *lacO* located outside the homologous flanking sequences (pSDM8001-*lacO*; Figure 10D). Upon co-cultivation of *Agrobacterium* carrying this vector with BY4741 or *ada2Δ* expressing LacI-GFP again only very few cells with fluorescent structures were seen. In one of the *ada2Δ* cells a fluorescent structure residing in the nucleus and in another cell in addition a single spot was observed (Figure 10D). We did not observe fluorescent structures in the BY4741 strain after checking a similar number of cells as for the *ada2Δ* mutant.

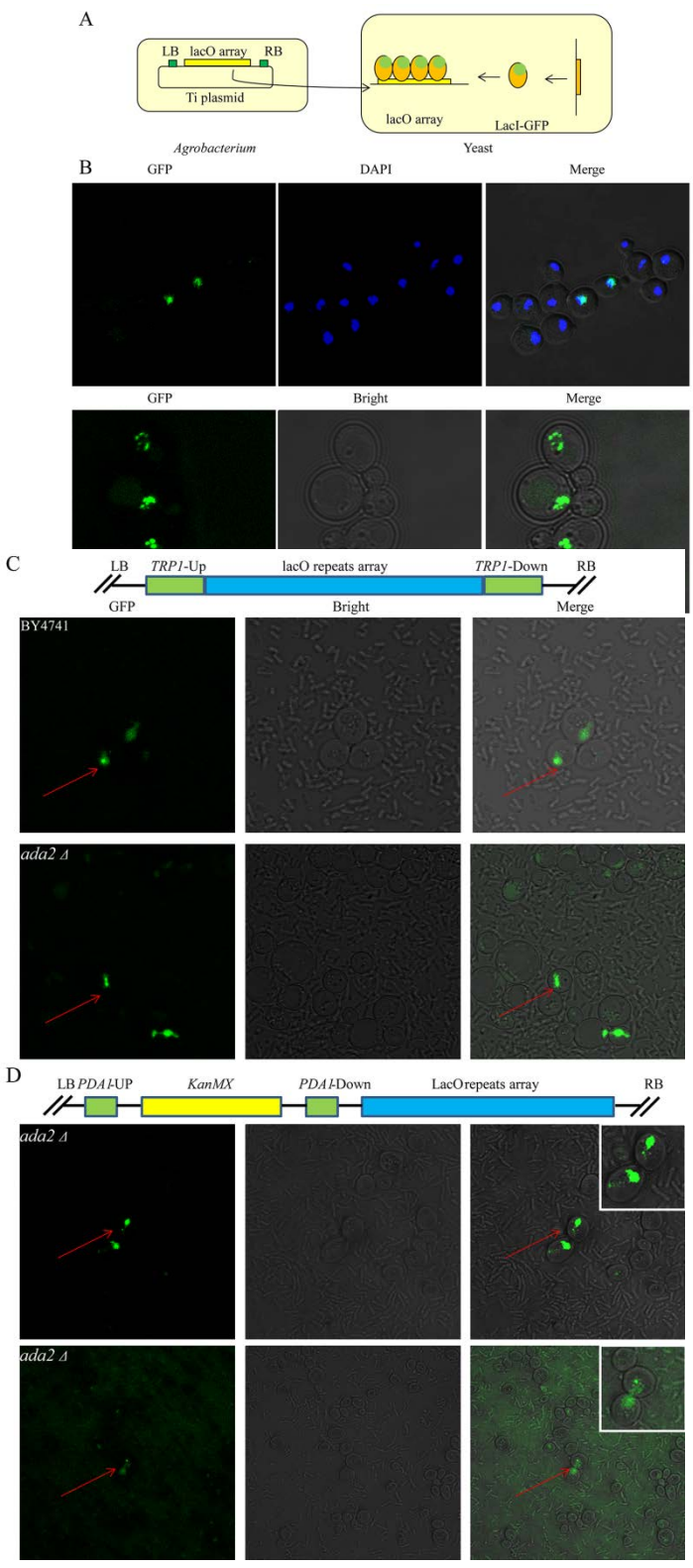

Figure 10. 256 *lacO*-LacI assay to visualize the fate of T-DNA after it has been delivered into recipient yeast cells. (A) Schematic of the 256 *lacO*-LacI assay. pRS305-LacI-GFP was integrated into the *LEU2* locus of yeast by homologous recombination so that LacI-GFP fusions can be expressed in the nucleus continuously. The T-DNA construct carries the 256 *lacO* repeat array and once it enters into the nucleus and has become double stranded, the *lacO* repeat array can recruit GFP–LacI fusions to form foci which can be monitored. (B) The high copy number plasmid pRS425 harboring the 256 *lacO* repeat array was introduced into the recipient yeast cells to test the stability of the 256 *lacO*-LacI assay. DAPI was used to visualize the nucleus of yeast cells. (C) The structure of T-DNA of plasmid pCAMBIA2300[trp1-lacO] is presented. *Agrobacterium* harboring this T-DNA was co-cultivated with wild type and *ada2Δ* deletion mutant cells expressing LacI-GFP. After 3 days, the mixture of *Agrobacterium* and yeast cells were washed three times with MilliQ water and were visualized using confocal microscopy. (D) A T-DNA construct harboring 256 *lacO* repeat array outside the flanking homologous sequences was used to visualize the fate of T-DNA which was not integrated into the desired locus.

Discussion

The bacterial side of AMT has been investigated rather well but about the host factors involved in this process less is known. The yeast *S. cerevisiae* has emerged as an excellent model host to

study the mechanism of AMT (Bundock et al, 1995; van Attikum et al., 2001, 2003; Zhang et al., 2017). Several large scale genome-wide screens have been used to find yeast host genes involved in this process (Soltani et al., 2009; Ohmine et al., 2016; Hooykaas et al., 2018). Previous research in our group revealed that in the *ada2Δ* deletion mutant the efficiency of AMT with a vector integrating via HR is higher than that in the wild type. In this chapter, we exploited the non-homologous T-DNA vector pRAL7102 to investigate AMT with a vector integrating by NHEJ in the *ada2Δ* deletion mutant. As shown in Figure 2 the AMT efficiency in the *ada2Δ* deletion mutant is highly increased not only when the T-DNA is integrated by HR but also when it is integrated by NHEJ.

It is unknown why deletion of *ADA2* results in an increased AMT efficiency. In the commonly used experimental procedures to check the efficiency of AMT, the initial ratio of donor *Agrobacterium* cells and recipient yeast cells is important for a high AMT efficiency. Ohmine et al., 2016 reported an observation that when recipient wild type yeast cells were overloaded with *Agrobacterium* or when a yeast mutant was used which could continue to grow in the presence of *Agrobacterium* to produce more cells than the wild type during the co-cultivation, the final AMT efficiency was attenuated. As the *ada2Δ* deletion mutant exhibits a slower growth and delayed cell cycle compared to the wild type, the ratio of *Agrobacterium* to yeast may be suboptimal. In our experiments, the initial amount of *ada2Δ* deletion mutant cells was almost identical with that of wild type cells. After co-cultivation the final output number of *ada2Δ* cells was lower (around half of that of wild type), thus contributing to an increased AMT efficiency.

An alternative way to explain the enhanced AMT efficiency may be that the observed effect is the result of the expression level of the selection marker. It has been reported that there may be a significant difference between the number of transformants obtained after selection and obtained without selection (Shilo et al., 2017). T-DNA integration does not necessarily lead to expression of the selection marker and it is possible that observed differences in AMT efficiency are caused by differences in the expression of the selection marker. In the AMT protocol used in this chapter stable expression of the selection marker was used to determine the efficiency of T-DNA integration. Thus, the increased AMT efficiency may be caused by an altered expression of the selection gene in the *ada2Δ* mutant when the T-DNA is inserted into a region of the chromosome that is silenced in the wild type and not in the *ada2Δ* mutant. In line with this hypothesis, the absence of *ADA2* was reported to facilitate the spread of heterochromatic proteins and to cause de-repression of a normally silenced telomere gene (Jacobson and Pillus, 2009). Moreover, T-DNA was reported to preferentially integrate at (sub)telomere regions in *rad50*, *mre11* and *xrs2* mutants (van Attikum et al., 2001). On the other hand, we have no evidence that silencing of the selection markers indeed plays a role in the AMT experiments shown in this chapter.

Simultaneously, the affected AMT efficiency could be the consequence of altered expression of certain genes directly or indirectly regulated by *ADA2*. The expression of approximately 2.5% of all yeast genes was found to be affected at least 2-fold by the *ada2Δ* deletion (Hoke et al., 2008). It can be speculated that the increased AMT efficiency of the *ada2Δ* deletion mutant is the consequence an indirect effect of the altered regulation of certain genes involved in the transformation process. Taking together, the increased AMT efficiency of *ada2Δ* deletion mutant can also be caused by an altered expression of genes other than *ADA2*.

It is well known that chromatin modifications play an crucial role in DNA repair mechanisms which are exploited to facilitate T-DNA integration. Several observations were described and reviewed (Magori and Citovsky, 2011), indicating that the histone acetylation balance is important for T-DNA integration even though its molecular basis remains unclear. *ADA2* is a component of histone acetyltransferase (HAT) complexes related to chromatin modifications and T-DNA integration was reported to be accompanied with chromosomal instability in *rad50*, *mre11*, *xrs2* and *lig4* mutants (van Attikum et al., 2001). Hence, another plausible hypothesis could be that genomic DNA surrounding DSBs would be more "open" and accessible thus serving as "hot spots" to be recognized for T-DNA integration during AMT and the increased AMT efficiency could be due to more emergent DNA damage events in the *ada2Δ* deletion mutant.

Deletion of *ADA2* renders yeast cells sensitive to various DNA damaging agents such as the drug methyl methanesulfonate (MMS) and the replication inhibitor hydroxyurea (HU). In order to gain more insight in the role of *ADA2* in the response to DNA damaging agents, we performed a synthetic rescue screen by using a YEp24-based genomic overexpression *S. cerevisiae* library. In this way, we identified *SFP1* and *HEM2* to rescue the *ada2Δ* deletion mutant in presence of MMS. However, the effect of overexpression of *HEM2* was not specific for the *ada2Δ* mutant as it has a similar effect on the wild type strain BY4741. Moreover *HEM2* was reported to be a potential target of MMS (Lum et al, 2004); therefore, we focused on the interaction between *SFP1* and *ADA2*. A physical interaction between Sfp1 and Ada2 has not yet been reported. Likewise, we were not able to show a physical interaction between Ada2 and Sfp1 in an yeast two-hybrid analysis in our lab. In addition, *sfp1Δ* deletion mutant grows very slowly and unusually small colonies were obtained (Jorgensen et al., 2002). We were unable to construct an *ada2Δsfp1Δ* double deletion mutant and this phenotype may be caused by synthetic lethality of *ada2Δsfp1Δ* double deletion, although this synthetic lethality has not been reported before (SGD, www.yeastgenome.org).

SFP1 overexpression was reported to influence the expression of over 30% of RNAPII-transcribed genes and Sfp1 can bind at G1/S gene promoters as a negative regulator (Albert et al., 2019). Similarly, Ada2 is a subunit of a transcription activator complex and thought to be involved in activation of RNA polymerase II transcription. In our studies, the *ada2Δ* deletion mutant grows slower and has a smaller cell size than the corresponding wild type (Figure 3) and the cell cycle of *ada2Δ* deletion mutant may be impaired (Figure 4). Considering the overlapping effects caused by manipulating *SFP1* and *ADA2* expression and the genetic interaction between these genes found in this study, it is very likely they participate in the same process. However, the nature of this process is so far unknown.

Recently, *SFP1* was identified to be involved in the regulation of Tra1 expression in response to polyQ proteotoxicity (Jiang et al., 2019). An interaction between *SFP1* and *TRA1* has been reported before and *SFP1* was postulated to be a negative and indirect regulator of *TRA1*, potentially through its regulation of the TORC1 complex (Lempiainen et al., 2009). Moreover, the expression of *TRA1* was upregulated by polyQ expansions in the absence of *ADA2*. Like Ada2, Tra1 is a key component of the SAGA histone acetyltransferase complex and Tra1 physically interacts with Ada2 (Saleh et al., 1998) and a synthetic lethal interaction between *ADA2* and *TRA1* has been found (Berg et al., 2018). In our study, overexpressed *TRA1* could not rescue the growth in the *ada2Δ* background in the presence of MMS (Figure S1). The

results suggest that the interaction between *SFP*1 and *ADA2* has no relevance to the role of *SFP1* in its regulation of TORC1 complex. It is consistent with the growth deficiency of *ada2Δ* deletion mutant no matter whether *SFP1* is overexpressed or not.

There is more evidence supporting a role of Sfp1 in the DSB repair pathway. For instance, *SFP1* was identified in a screen using diploid yeast deletion strain libraries for sensitivity to various DSB agents, such as MMS, bleomycin and *Eco*RI (McKinney et al., 2013). However, which role *SFP1* may have in DSB repair has not been elucidated. Meanwhile, in a proteome-wide study, a physical interaction has been reported between Sfp1 and Asf1 (Krogan et al., 2006). Asf1 is a nucleosome assembly factor, involved in chromatin assembly and disassembly and required for recovery after DSB repair, although the functional significance of the interaction with Sfp1 has not been established. In this chapter, we demonstrated that the *ada2Δ* mutant is sensitive to DNA damaging agents such as MMS and HU and that overexpression of *SFP1* in the *ada2Δ* background specifically suppressed MMS sensitivity. These findings define a genetic interaction between *SFP1* and *ADA2* in the DNA damage response which is separate from the function of *SFP1* in the regulation of ribosomal protein and biogenesis genes.

Besides such indirect roles of *ADA2* in gene expression or chromatin structure, we need also to consider that there is more DNA damage in the *ada2Δ* deletion mutant as revealed by an increased number of *RAD52* foci. Due to the absence of *ADA2*, there are either more DNA damaging events in the cell or this damage is repaired less efficiently, thus providing more available sites for T-DNA integration. The increased DNA damage events could be expected to occur at random chromosomal loci and a small portion of them may be at or near the desired locus for T-DNA HR integration. Correspondingly, as described above the AMT efficiency by NHEJ increased 50 fold, while that by HR was only 2 fold higher in the absence of *ADA2* compared to the wildtype strain (Table S1B). Overexpression of *SFP1* in the *ada2Δ* deletion background not only reduces MMS sensitivity and the occurrence of DNA damage (the number of *RAD52* foci is less than 5 per 100 cells in the absence of MMS), but also leads to a reduction in AMT to wildtype levels. Thus, the increased AMT efficiency of the *ada2Δ* mutants together with the genetic interaction between *ADA2* and *SFP1* in response to DNA damaging agents suggest an important role of DNA damage events in T-DNA integration in the *ada2Δ* mutant.

Acknowledgements

We would like to thank Andrew W Murray (Harvard University) for plasmids pAFS59 and pAFS152, Christopher Korch (University of Umea) for YEp24 overexpression library, Xiaorong Zhang (our group) for strain W303 *bar1Δ*, and Gerda Lamers (our institute) for technical support on microscopy.

Table 1. Yeast strains used in this study.

Yeast strain	Genotype	Source/Reference
BY4741	MATa *his3Δ1 leu2Δ0 met15Δ0 ura3Δ0*	Brachmann et al., 1998
BY4741 *ada2Δ*	MATa *his3Δ1 leu2Δ0 met15Δ0 ura3Δ0 ada2*::HphMX4	This study
BY4741 *gcn5Δ*	MATa *his3Δ1 leu2Δ0 met15Δ0 ura3Δ0 gcn5*::HphMX4	This study
BY4741-Rad52-GFP	BY4741 Rad52-GFP (KanMX4)	This study
BY4741 *ada2Δ*-Rad52-GFP	BY4741 *ada2*::HphMX4 Rad52-GFP	This study
BY4741 YEp24	BY4741 YEp24	This study
BY4741 YEp24::SFP1	BY4741 YEp24::SFP1	This study
BY4741 *ada2Δ* YEp24	BY4741 *ada2*::HphMX4 YEp24	This study
BY4741 *ada2Δ* YEp24::SFP1	BY4741 *ada2*::HphMX4 YEp24::SFP1	This study
BY4741 *gcn5Δ* YEp24	BY4741 *gcn5*::HphMX4	This study
BY4741 *gcn5Δ* YEp24::SFP1	BY4741 *gcn5*::HphMX4 YEp24::SFP1	This study
BY4741-LacI-GFP	BY4741 *leu2*::LacI-GFP	This study
BY4741 *ada2Δ*-LacI-GFP	BY4741 *ada2*::HphMX4 *leu2*::LacI-GFP	This study
BY4741 pUG34-SFP1	BY4741 pUG34::SFP1	This study
BY4741 *ada2Δ* pUG34-SFP1	BY4741 *ada2*::HphMX4 pUG34::SFP1	This study
W303a	MATa *leu2-3,112 trp1-1 can1-100 ura3-1 ade2-1 his3-11,15*	Thomas and Rothstein, 1989
W303a-lacO-LacI	W303a *ura3-1*::LacI-GFP pRS425::*lacO*256	This study
BY4741-lacO-LacI	BY4741 *ura3Δ*0::LacI-GFP pRS425::*lacO*256	This study
W303a *bar1Δ*	W303a *bar1*:: KanMX4	Zhang et al., 2017
W303a *bar1Δ ada2Δ*	W303a *bar1*:: KanMX4 *ada2*::HphMX4	This study

Table 2. Plasmids used in this study.

Plasmids	Specifications	Source/Reference
pAG32	contains the *hph* gene encoding hygromycin B phosphotransferase	Goldstein and McCusker, 1999
pUG6	contains the kanMX gene encoding kanamycin cassette	Güldener et al, 1996
pYM27	PCR template for C-terminal EGFP tagging	Janke et al., 2004
YEp24	Yeast episomal cloning vector with a *URA3* marker	Carlson and Botstein,1982
YEp24-SFP1	YEp24 with the coding sequence of *SFP1*	This study
pAFS59	Yeast integrative vector harboring 256 *lacO* repeats	Straight et al., 1996
pAFS152	Yeast integrative vector harboring LacI-GFP fusions	Straight et al., 1996
pRS305	Yeast integrative vector with a *LEU2* marker	Sikorski and Hieter, 1989
pRS305-LacI-GFP	pRS305 with LacI-GFP fusion protein	This study
pRS425	Yeast episomal expression vector with a *LEU2* marker	Sikorski and Hieter, 1989
pRS425[*lacO*]	pRS425 with *lacO* repeat array	This study

pRS425[SFP1]	pRS425 with the coding sequence of *SFP1*	This study
pCAMBIA2300	*Agrobacterium* binary vector for transformation, Km	Hajdukiewicz et al., 1994
pCAMBIA2300[*trp1*]		
pCAMBIA2300-*lacO*	pCAMBIA2300 with *lacO* repeat array	This study
pCAMBIA2300[*trp1-lacO*]	pCAMBIA2300 with *lacO* repeat array and *TRP1* flanking sequence	This study
pCAMBIA2300[*trp1*-kanMX]	pCAMBIA2300 with KanMX marker and *TRP1* flanking sequence	This study
pRAL7100	*Agrobacterium* binary vector with *URA3* selectable marker and PDA1 flanking sequence	Bundock et al., 1995
pRAL7102	*Agrobacterium* binary vector with *URA3* selectable marker	Bundock and Hooykaas, 1996
pSDM8001	*Agrobacterium* binary vector with KanMX selectable marker and *PDA1* flanking sequence	van Attikum and Hooykaas, 2003
pSDM8001-*lacO*	pSDM8001 containing *lacO* repeat array between PDA1 and right border	This study
pUG34	Centromeric plasmid with a *HIS3* marker for N-terminal GFP fusions under control of the *MET25* promoter	Guldener and Hegemann, unpublished
pUG34-*SFP1*	pUG34 with the coding sequence of *SFP1*	This study
Yeast Genomic Tiling Collection	complete overlapping collection of entire *S. cerevisiae* genome, screen for overexpression phenotypes	Dharmacon

Table 3. Primers used in this study.

primer name	sequence (5'-3')
Ada2-Fw	TAAAATATCAGCGTAGTCTGAAAATATATACATTAAGCAAAAAGACAGCTGAAGCTTCGTACGC
Ada2-Rev	ATAATAACTAGTGACAATTGTAGTTACTTTTCAATTTTTTTTTTGCCGCGGCCGCATAGGCCAC
Ada2-Ctrol-Fw	ACGACCTCTGAGAAAACGA
Ada2-Ctrol-Rev	GGTCCCTTTATGACTTGGC
Ada2-gfp-Fw	GCGAATAGAATATACGATTTTTTCCAGAGCCAGAATTGGATGCGTACGCTGCAGGTCGAC
Ada2-gfp-Rev	TAGTGACAATTGTAGTTACTTTTCAATTTTTTTTTTGTTAACTATAGGGAGACCGGCAGATCCGC
Rad52-gfp-Fw	AGAGAAGTTGGAAGACCAAAGATCAATCCCCTGCATGCACGCAAGCCTACTCGTACGCTGCAGGTC
Rad52-gfp-Rev	AGTAATAAATAATGATGCAAATTTTTTATTTGTTTCGGCCAGGAAGCGTTTCAATCGATGAATTCGA
Trp1-up-Fw	AAGAGCTCAAAACGGAAGAGGAGTAGGG
Trp1-up-Rev	AAGGATCCTGCTTAATCACGTATACTCACG
Trp1-down-Fw	AACTGCAGAGGCCTTTTGAAAAGCAAGCA
Trp1-down-Rev	AAAAGCTTTACTTGACGACTTGAGGCTG
LacI-Fw	ACTAGTGTTTTCCCAGTCACGACGTT
LacI-Rev	GTCGACACGCCAAGCTCGGAATTAAC
SFP1-Fw/YEp24	CTAGCTAGCTTACCTCCCAGGCCCTATCT
LSB6-Fw	CTAGCTAGCAAGGTTTCCAGCCACAGTTG
GDS1-Fw	CTAGCTAGCAACCCATGCGATGAGAAGTC
CIR2-Fw	CATGCATGCTCCGACATCAATTCCAGTCA

HEM2-Fw	CATGCATGCAGAAATGACTGCCTGGTGCT
SNX3-Fw	CATGCATGCTCCTGTACCATCCGGAACTC
SFP1-Rev/YEp24	ACGCGTCGACAGAAAAACGATCCGACAACG
LSB6-Rev	ACGCGTCGACGGGACCTAGTCCAACATTGC
GDS1-Rev	ACGCGTCGACTCCCAGAGTGGATTTTCCTG
CIR2-Rev	ACGCGTCGACTGCTGTCAAAAGGACATGGA
HEM2-Rev	ACGCGTCGACATCTTGGGACGACAGACAGC
SNX3-Rev	ACGCGTCGACCGGGAAACTTGGTGGATATG
SFP1-pUg34-Fw	TCCCCCGGGGATTTTACAACAATGACTATGGC
SHP1-pUg34-Rev	ACGCGTCGACTTAGTGAGTGGAGTGGCCCCTGTG
MRS6-Fw	TCCCCCGGGTGTGCTTATCGGGGGTCTAC
MRS6-Rev	ACGCGTCGACAGACCATCGTGAACCAAAGC
LST8-Fw	CGCGGATCCAGCAGCCTCGAGACCGTAT
LST8-Rev	ACGCGTCGACGAAGAGCGTTTGAAGGCAAG
TCO89-Fw	CGCGGATCCCCTACGACCATCGAAAGAGC
TCO89-Rev	TCCCCCGGGGGGCTTTAGCGACAGAAACA
SEA4-Fw	AACTGCAGCGCTTACATGCAACGTTTTG
SEA4-Rev	ACGCGTCGACATCTTCGCTGCCATTTTCAC
VAM6-Fw	CGCGGATCCGTTGGCGCCATGTGTGTATT
VAM6-Rev	ACGCGTCGACGAACACCAGCCGGTATTAGC
LST7-Fw	AACTGCAGTACAAAGTCATCGCCAGCAG
LST7-Rev	ACGCGTCGACCGGTGATAACGATGGGAAAG
GTR2-Fw	CGCGGATCCTTTCAGAAGGGACGCTCCTC
GTR2-Rev	ACGCGTCGACTTCTTCGGGTGTTGTCTTCC
TOR1-Fw	AACTGCAGCCATGTGATCCCAATTTTCC
TOR1-Rev	ACGCGTCGACGCAAGAGGGGGTACTTGGAC
LST4-Fw	CGCGGATCCTGTGGGCAATTGGGTGTACT
LST4-Rev	ACGCGTCGACGATAACGGCCAAATGAAACG
GTR1-Fw	AACTGCAGTTTTCAGCCGGGCAACATTT
GTR1-Rev	ACGCGTCGACCCAAGTAGCGCACCAAGAGG
URA3-A	TGCACGAAAAGCAAACAAAC
URA3-B	AATGCGTCTCCCTTGTCATC
URA3-C	GAAGGTTAATGTGGCTGTGG
URA3-D	TTGGTTCTGGCGAGGTATTG

The sequences of restriction enezymes are underlined.

Table S1.

A. Frequencies of T-DNA integration by homologous recombination in yeast cells.

Yeast	*Agrobacterium*	Frequency of Ura$^+$ colonies per output recipient (mean ± SD, n=3)
W303a		$1.4 \pm 0.04 \times 10^{-5}$
BY4743	LBA1100 pRAL7100	$1.2 \pm 0.2 \times 10^{-4}$
BY4741		$9.7 \pm 0.3 \times 10^{-5}$

B. Frequencies of T-DNA integration by homologous recombination and non-homologous end-joining in yeast cells.

Yeast	*Agrobacterium*	Frequency of positive colonies per output recipient (mean ± SD, n=3)
BY4741	LBA1100 pRAL7100	$1.1 \pm 0.6 \times 10^{-4}$
BY4741 *ada2ΔΔ*		$4.4 \pm 0.8 \times 10^{-4}$
BY4741	LBA1100 pCAMBIA2300[*trp1*-kanMx]	$0.6 \pm 0.3 \times 10^{-4}$
BY4741 *ada2Δ*		$1.2 \pm 0.7 \times 10^{-4}$
BY4741	LBA1100 pRAL7102	$2.4 \pm 1.4 \times 10^{-6}$
BY4741 *ada2Δ*		$1.0 \pm 0.2 \times 10^{-4}$

C. Effect of the absence of *ADA2* on the fraction of transformants surviving on plates supplemented with FAA[a].

	Experiment			Average percentage ±	P value
BY4741	6/198 (3.03)[b]	8/386 (2.07)	9/404 (2.22)	2.4 ± 0.5	0.00141
ada2Δ	45/209 (21.53)	156/482 (32.37)	44/157 (28.03)	27.3 ± 5.4	

a. The transformants were first selected for G418 resistance and were subsequently streaked on plates with or without FAA. Transformants with the T-DNA integrated in the *TRP1* locus are expected to grow on media with FAA.

b. The percentage of surviving transformants is given in parentheses. All yeast cells were transformed by the derivatives of *Agrobacterium* strain LBA1100 with corresponding T-DNA vectors listed in the table. The frequencies were calculated as the number of positive colonies divided by the whole output number of yeast cells and the average value of at least three independent experiments is shown.

Table S2. Selected genes involved in the TORC1 pathway for synthetic rescue studies.

Gene	Description of encoded protein
MRS6	rab escort protein
SCH9	required for TORC1-mediated regulation
KOG1	subunit of TORC1
TRA1	subunit of SAGA complex
TOR1	subunit of TORC1
LST8	component of the TOR signaling pathway
RPC82	subunit of RNA polymerase III
MOT1	protein involved in regulation of transcription
TCO89	subunit of TORC1
RAP1	DNA-binding transcription regulator
IFH1	coactivator of ribosomal protein genes
FHL1	Regulator of ribosomal protein transcription
GCR2	transcriptional activator of genes involved in glycolysis
GCR1	transcriptional activator of genes involved in glycolysis
YMR111C	enriches ubiquitin on chromatin
EGO2	subunit of the EGO/GSE complex
NPR3	nitrogen permease regulator
SEA4	subunit of the SEA complex
VAM6	vacuole membrane protein
MTC5	maintenance of telomere capping
SEH1	subunit of the SEA complex
LST7	subunit of the Lst4p-Lst7p GTPase complex for Gtr2p
GTR2	subunit of a TORC1-stimulating GTPase
LST4	subunit of the Lst4p-Lst7p GTPase complex for Gtr2p
SEC13	subunit of the SEA complex
GTR1	subunit of a TORC1-stimulating GTPase
RTC1	subunit of the SEA complex

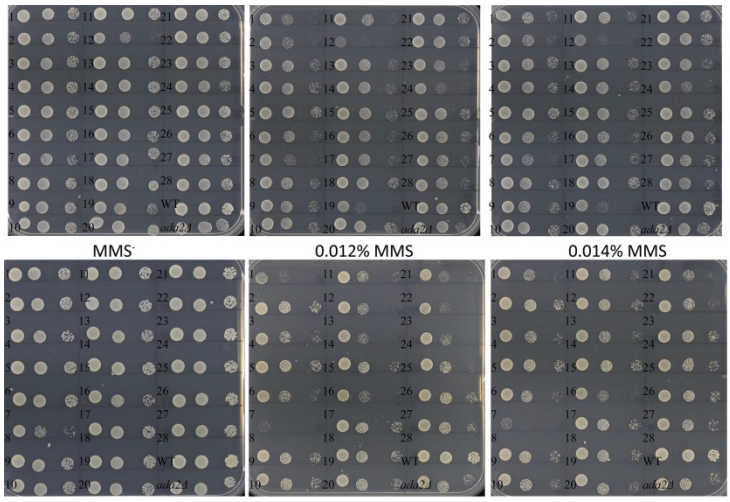

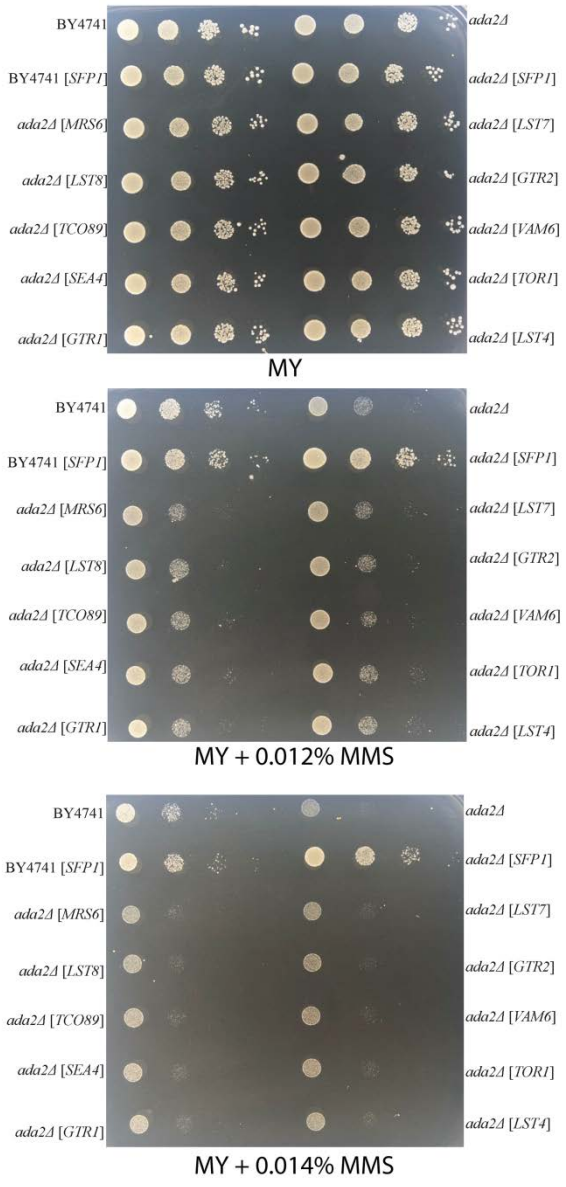

Figure S1. MMS sensitivity of *ada2Δ* deletion mutant could not be rescued by overexpression of genes related to the TORC pathway. (A) 27 candidate genes were selected to test whether overexpression of them can enhance or reduce sensitivity to MMS in the *ada2Δ* deletion mutant. These genes are involved in the TORC pathway or the regulation of TORC1 signaling. Overexpression vectors harboring these genes were obtained from the Yeast Genomic Tiling Collection and introduced into the *ada2Δ* deletion mutant via the LiAc method. (B) Each single candidate gene including its promoter region was cloned into high copy vector pRS425 and introduced into the *ada2Δ* deletion mutant to test the sensitivity to MMS. The vectors pRS425 and pRS425[SFP1] were introduced as controls. All mutants were serially diluted and spotted onto MY medium with the indicated concentrations of MMS. After 3 days, the photos were taken and the spot assays were performed at least three independent times.

References

Albert, B., Tomassetti, S., Gloor, Y., Dilg, D., Mattarocci, S., Kubik, S., & Shore, D. (2019). Sfp1 regulates transcriptional networks driving cell growth and division through multiple promoter-binding modes. *Genes & development*, 33, 288-293.

Anand, A., Vaghchhipawala, Z., Ryu, C. M., Kang, L., Wang, K., del-Pozo, Olga., Martin, G. B., & Mysore, K. S. (2007). Identification and characterization of plant genes involved in *Agrobacterium*-mediated plant transformation by virus-induced gene silencing. *Molecular plant-microbe interactions*, 20, 41–52.

Balasubramanian, R., Pray-Grant, M. G., Selleck, W., Grant, P. A., & Tan, S. (2002). Role of the Ada2 and Ada3 transcriptional coactivators in histone acetylation. *Journal of Biological Chemistry*, 277, 7989-7995.

Baudin, A., Ozier-Kalogeropoulos, O., Denouel, A., Lacroute, F., & Cullin, C. (1993). A simple and efficient method for direct gene deletion in *Saccharomyces cerevisiae*. *Nucleic acids research*, 21, 3329.

Beijersbergen, A., Den Dulk-Ras, A., Schilperoort, R. A., & Hooykaas, P. J. J. (1992). Conjugative transfer by the virulence system of *Agrobacterium tumefaciens*. *Science*, 256, 1324-1327.

Berger, S. L., Piña, B., Silverman, N., Marcus, G. A., Agapite, J., Regier, J. L., Triezenberg, S. J., & Guarente, L. (1992) Genetic isolation of ADA2: A potential transcriptional adaptor required for function of certain acidic activation domains. *Cell*, 70, 251-265

Berg, M. D., Genereaux, J., Karagiannis, J., & Brandl, C. J. (2018). The pseudokinase domain of *Saccharomyces cerevisiae* Tra1 is required for nuclear localization and incorporation into the SAGA and NuA4 complexes. *G3: Genes, Genomes, Genetics*, 8, 1943-1957.

Brachmann, C. B., Davies, A., Cost, G. J., Caputo, E., Li, J., Hieter, P., & Boeke, J. D. (1998). Designer deletion strains derived from *Saccharomyces cerevisiae* S288C: a useful set of strains and plasmids for PCR-mediated gene disruption and other applications. *Yeast*, 14, 115-132.

Bundock, P., den Dulk-Ras, A., Beijersbergen, A., & Hooykaas, P. J. J. (1995). Trans-kingdom T-DNA transfer from *Agrobacterium tumefaciens* to *Saccharomyces cerevisiae*. *The EMBO journal*, 14, 3206-3214.

Bundock, P., & Hooykaas, P. J. J. (1996). Integration of *Agrobacterium tumefaciens* T-DNA in the *Saccharomyces cerevisiae* genome by illegitimate recombination. *Proceedings of the National Academy of Sciences*, 93, 15272-15275.

Carlson, M., & Botstein, D. (1982). Two differentially regulated mRNAs with different 5′ ends encode secreted and intracellular forms of yeast invertase. *Cell*, 28, 145-154.

Christie, P. J., & Gordon, J. E. (2014). The *Agrobacterium* Ti plasmids. *Microbiology spectrum*, 2, 1-18.

Crane, Y. M., & Gelvin, S. B. (2007). RNAi-mediated gene silencing reveals involvement of *Arabidopsis* chromatin-related genes in *Agrobacterium*-mediated root transformation. *Proceedings of the National Academy of Sciences*, 104, 15156-15161.

De Groot, M. J., Bundock, P., Hooykaas, P. J. J., & Beijersbergen, A. G. (1998). *Agrobacterium* tumefaciens-mediated transformation of filamentous fungi. *Nature biotechnology*, 16, 839.

den Dulk-Ras, A., & Hooykaas, P. J. J. (1995). Electroporation of *Agrobacterium tumefaciens*. In *Plant Cell Electroporation and Electrofusion Protocols*, 63-72. Springer, Totowa, NJ.

Gietz, R. D., Schiestl, R. H., Willems, A. R., & Woods, R. A. (1995). Studies on the transformation of intact yeast cells by the LiAc/SS-DNA/PEG procedure. *Yeast*, 11, 355-360.
Grant, P. A., Duggan, L., Côté, J., Roberts, S. M., Brownell, J. E., Candau, R., Ohba, R., Owen-Hughes, T., Allis, C. D., Winston, F., Berger, S. L., & Workman J. L. (1997). Yeast Gcn5 functions in two multisubunit complexes to acetylate nucleosomal histones: characterization of an Ada complex and the SAGA (Spt/Ada) complex. *Genes & development*, 11, 1640-1650.
Gelvin, S. B. (2003). *Agrobacterium*-mediated plant transformation: the biology behind the "gene-jockeying" tool. *Microbiology and molecular biology reviews*, 67, 16-37.
Gelvin, S. B. (2017). Integration of *Agrobacterium* T-DNA into the plant genome. *Annual review of genetics*, 51, 195-217.
Goldstein, A. L., & McCusker, J. H. (1999). Three new dominant drug resistance cassettes for gene disruption in *Saccharomyces cerevisiae*. *Yeast*, 15, 1541-1553.
Güldener, U., Heck, S., Fiedler, T., Beinhauer, J., & Hegemann, J. H. (1996). A new efficient gene disruption cassette for repeated use in budding yeast. *Nucleic acids research*, 24, 2519-2524.
Hajdukiewicz, P., Svab, Z., & Maliga, P. (1994). The small, versatile pPZP family of *Agrobacterium* binary vectors for plant transformation. *Plant molecular biology*, 25, 989-994.
Hark, A. T., Vlachonasios, K. E., Pavangadkar, K. A., Rao, S., Gordon, H., Adamakis, I. D., Kaldis, A., Thomashow, M. F., & Triezenberg, S. J. (2009). Two *Arabidopsis* orthologs of the transcriptional coactivator ADA2 have distinct biological functions. *Biochimica et Biophysica Acta (BBA)-Gene Regulatory Mechanisms*, 1789, 117-124.
Hoke, S. M., Genereaux, J., Liang, G., & Brandl, C. J. (2008). A conserved central region of yeast Ada2 regulates the histone acetyltransferase activity of Gcn5 and interacts with phospholipids. *Journal of molecular biology*, 384, 743-755.
Hooykaas, P. J. J., van Heusden, G. P. H., Niu, X., Roushan, M. R., Soltani, J., Zhang, X., & van der Zaal, B. J. (2018). Agrobacterium-mediated transformation of yeast and fungi. *Current Topics in Microbiology and Immunology*, 418, 349-374.
Jacobson, S., & Pillus, L. (2009). The SAGA subunit Ada2 functions in transcriptional silencing. *Molecular and cellular biology*, 29, 6033-6045.Janke, C., Magiera, M. M., Rathfelder, N., Taxis, C., Reber, S., Maekawa, H., Moreno - Borchart, A., Doenges, G., Schwob, E., Schiebel, E., & Knop, M. (2004). A versatile toolbox for PCR-based tagging of yeast genes: new fluorescent proteins, more markers and promoter substitution cassettes. *Yeast*, 21, 947-962.
Jiang, Y., Berg, M. D., Genereaux, J., Ahmed, K., Duennwald, M. L., Brandl, C. J., & Lajoie, P. (2019). Sfp1 links TORC1 and cell growth regulation to the yeast SAGA-complex component Tra1 in response to polyQ proteotoxicity. *Traffic*, 20, 267-283.
Jorgensen, P., Nishikawa, J. L., Breitkreutz, B. J., & Tyers, M. (2002). Systematic identification of pathways that couple cell growth and division in yeast. *Science*, 297, 395-400.
Jorgensen, P., Rupeš, I., Sharom, J. R., Schneper, L., Broach, J. R., & Tyers, M. (2004). A dynamic transcriptional network communicates growth potential to ribosome synthesis and critical cell size. *Genes & development*, 18, 2491-2505.
Krogan, N. J., Cagney, G., Yu, H., Zhong, G., Guo, X., Ignatchenko, A., & Punna, T. (2006). Global landscape of protein complexes in the yeast *Saccharomyces cerevisiae*. *Nature*, 440, 637.
Lai, J., Jiang, J., Wu, Q., Mao, N., Han, D., Hu, H., & Yang, C. (2018). The transcriptional coactivator ADA2b recruits a structural maintenance protein to double-strand breaks during DNA repair in plants. *Plant physiology*, 176, 2613-2622.

Lempiäinen, H., Uotila, A., Urban, J., Dohnal, I., Ammerer, G., Loewith, R., & Shore, D. (2009). Sfp1 interaction with TORC1 and Mrs6 reveals feedback regulation on TOR signaling. *Molecular cell*, 33, 704-716.

Leung, G. P., Lee, L., Schmidt, T. I., Shirahige, K., & Kobor, M. S. (2011). Rtt107 is required for recruitment of the SMC5/6 complex to DNA double-strand breaks. *Journal of Biological Chemistry*, 286, 26250-26257.

Lisby, M., Rothstein, R., & Mortensen, U. H. (2001). Rad52 forms DNA repair and recombination centers during S phase. *Proceedings of the National Academy of Sciences*, 98, 8276-8282.

Lum, P. Y., Armour, C. D., Stepaniants, S. B., Cavet, G., Wolf, M. K., Butler, J. S., Hinshaw, J. C., Garnier, P., Prestwich, G. D., Leonardson, A., Garrett-Engele, P., Rush, C. M., Bard, M., Schimmack, G., Phillips, J. W., Roberts, C. J., & Shoemaker, D. D. (2004). Discovering modes of action for therapeutic compounds using a genome-wide screen of yeast heterozygotes. *Cell*, 116, 121-137.

Luo, Y., Chen, Z., Zhu, D., Tu, H., & Pan, S. Q. (2015). Yeast actin-related protein ARP6 negatively regulates *Agrobacterium*-mediated transformation of yeast cell. *BioMed research international*, 2015, 275092.

MacKay, V. L., Welch, S. K., Insley, M. Y., Manney, T. R., Holly, J., Saari, G. C., & Parker, M. L. (1988). The Saccharomyces cerevisiae BAR1 gene encodes an exported protein with homology to pepsin. *Proceedings of the National Academy of Sciences*, 85, 55-59.

Magori, S., & Citovsky, V. (2011). Epigenetic control of *Agrobacterium* T-DNA integration. *Biochimica et Biophysica Acta (BBA)-Gene Regulatory Mechanisms*, 1809, 388-394.

Marion, R. M., Regev, A., Segal, E., Barash, Y., Koller, D., Friedman, N., & O'Shea, E. K. (2004). Sfp1 is a stress-and nutrient-sensitive regulator of ribosomal protein gene expression. *Proceedings of the National Academy of Sciences*, 101, 14315-14322.

McKinney, J. S., Sethi, S., Tripp, J. D., Nguyen, T. N., Sanderson, B. A., Westmoreland, J. W., Resnick. M. A., & Lewis, L. K. (2013). A multistep genomic screen identifies new genes required for repair of DNA double-strand breaks in *Saccharomyces cerevisiae*. *BMC genomics*, 14, 251.

Muñoz-Galván S, Jimeno S, Rothstein R, Aguilera A (2013) Histone H3K56 Acetylation, Rad52, and Non-DNA Repair Factors Control Double-Strand Break Repair Choice with the Sister Chromatid. *PLoS Genetics*, 9, e1003237

Muratoglu, S., Georgieva, S., Pápai, G., Scheer, E., Enünlü, I., Komonyi, O., Cserpan, I., Lebedeva, L., Nabirochjina, E., Udvardy, A., Tora, L., & Boros, I. (2003). Two different *Drosophila* ADA2 homologues are present in distinct GCN5 histone acetyltransferase-containing complexes. *Molecular and cellular biology*, 23, 306-321.

Mysore, K. S., Nam, J., & Gelvin, S. B. (2000). An Arabidopsis histone H2A mutant is deficient in *Agrobacterium* T-DNA integration. *Proceedings of the National Academy of Sciences*, 97, 948-953.

Nester, E. W., Gordon, M. P., Amasino, R. M., & Yanofsky, M. F. (1984). Crown gall: a molecular and physiological analysis. *Annual Review of Plant Physiology*, 35, 387-413.

Niu, X., Zhou, M., Henkel, C. V., van Heusden, G. P. H., & Hooykaas, P. J. (2015). The *Agrobacterium tumefaciens* virulence protein VirE3 is a transcriptional activator of the F-box gene VBF. *The Plant Journal*, 84, 914-924.

Offringa, R., De Groot, M. J., Haagsman, H. J., Does, M. P., Van Den Elzen, P. J., & Hooykaas, P. J. J. (1990). Extrachromosomal homologous recombination and gene targeting in plant cells after *Agrobacterium* mediated transformation. *The EMBO journal*, 9, 3077-3084.

Ohmine, Y., Satoh, Y., Kiyokawa, K., Yamamoto, S., Moriguchi, K., & Suzuki, K. (2016). DNA repair genes RAD52 and SRS2, a cell wall synthesis regulator gene SMI1, and the membrane sterol synthesis scaffold gene ERG28 are important in efficient *Agrobacterium*-mediated yeast transformation with chromosomal T-DNA. *BMC microbiology*, 16, 58.

Păcurar, D. I., Thordal-Christensen, H., Păcurar, M. L., Pamfil, D., Botez, C., Bellini, C. (2011). *Agrobacterium tumefaciens*: From crown gall tumors to genetic transformation. *Physiological and molecular plant pathology*, 76, 76-81.

Rolloos, M., Dohmen, M. H., Hooykaas, P. J. J., & van der Zaal, B. J. (2014). Involvement of Rad52 in T-DNA circle formation during *Agrobacterium* tumefaciens-mediated transformation of *Saccharomyces cerevisiae*. *Molecular microbiology*, 91, 1240-1251.

Saleh, A., Schieltz, D., Ting, N., McMahon, S. B., Litchfield, D. W., Yates, J. R., Lees-Miller, S. P., Cole, M.D., & Brandl, C. J. (1998). Tra1p is a component of the yeast Ada Spt transcriptional regulatory complexes. *Journal of Biological Chemistry*, 273, 26559-26565.

Schindelin, J., Arganda-Carreras, I., Frise, E., Kaynig, V., Longair, M., Pietzsch, T., Preibisch, S., Rueden, C., Saalfeld, S., Schmid, B., Tinevez, J. Y., White, D. J., Hartenstein, V., Eliceiri, K., Tomancak, P., & Cardona, A. (2012). Fiji: an open-source platform for biological-image analysis. *Nature methods*, 9, 676.

Schrammeijer, B., Risseeuw, E., Pansegrau, W., Regensburg-Tuïnk, T. J., Crosby, W. L., & Hooykaas, P. J. (2001). Interaction of the virulence protein VirF of *Agrobacterium tumefaciens* with plant homologs of the yeast Skp1 protein. *Current Biology*, 11, 258-262.

Shilo, S., Tripathi, P., Melamed-Bessudo, C., Tzfadia, O., Muth, T. R., & Levy, A. A. (2017). T-DNA-genome junctions form early after infection and are influenced by the chromatin state of the host genome. *PLoS genetics*, 13, e1006875.

Sikorski, R. S., & Hieter, P. (1989). A system of shuttle vectors and yeast host strains designed for efficient manipulation of DNA in *Saccharomyces cerevisiae*. *Genetics*, 122, 19-27.

Singer, K., Shiboleth, Y. M., Li, J., & Tzfira, T. (2012). Formation of complex extrachromosomal T-DNA structures in *Agrobacterium*-infected plants. *Plant physiology*, 160, 511-522.

Soltani, J. (2009). Host genes involved in *Agrobacterium*-mediated transformation. Ph.D. thesis, Leiden University, Leiden, The Netherlands.

Soltani, J., Van Heusden, G. P. H., Hooykaas, P. J. J. (2009). Deletion of host histone acetyltransferases and deacetylases strongly affects *Agrobacterium*-mediated transformation of *Saccharomyces cerevisiae*. *FEMS microbiology letters*, 298, 228-233.

Sterner, D. E., Wang, X., Bloom, M. H., Simon, G. M., & Berger, S. L. (2002). The SANT domain of Ada2 is required for normal acetylation of histones by the yeast SAGA complex. *Journal of Biological Chemistry*, 277, 8178-8186.

Straight, A. F., Belmont, A. S., Robinett, C. C., & Murray, A. W. (1996). GFP tagging of budding yeast chromosomes reveals that protein–protein interactions can mediate sister chromatid cohesion. *Current Biology*, 6, 1599-1608.

Sun, J., Paduch, M., Kim, S. A., Kramer, R. M., Barrios, A. F., Lu, V., Luke, J., Usatyuk, S., Kossiakoff, A. A., & Tan, S. (2018). Structural basis for activation of SAGA histone

acetyltransferase Gcn5 by partner subunit Ada2. *Proceedings of the National Academy of Sciences*, 115, 10010-10015.
Thomas, B. J., & Rothstein, R. (1989). Elevated recombination rates in transcriptionally active DNA. *Cell*, 56, 619-630.
Toyn, J. H., Gunyuzlu, P. L., Hunter White, W., Thompson, L. A., & Hollis, G. F. (2000). A counterselection for the tryptophan pathway in yeast: 5-fluoroanthranilic acid resistance. *Yeast*, 16, 553-560.
Tzfira, T., Vaidya, M., & Citovsky, V. (2001). VIP1, an Arabidopsis protein that interacts with *Agrobacterium* VirE2, is involved in VirE2 nuclear import and *Agrobacterium* infectivity. *The EMBO Journal*, 20, 3596-3607.
Tzfira, T., & Citovsky, V. (2006). *Agrobacterium*-mediated genetic transformation of plants: biology and biotechnology. *Current opinion in biotechnology*, 17, 147-154.
Van Attikum, H., Bundock, P., & Hooykaas, P. J. J. (2001). Non-homologous end-joining proteins are required for *Agrobacterium* T-DNA integration. *The EMBO journal*, 20, 6550-6558.
Van Attikum, H., & Hooykaas, P. J. J. (2003). Genetic requirements for the targeted integration of *Agrobacterium* T-DNA in Saccharomyces cerevisiae. *Nucleic acids research*, 31, 826-832.
Van Kregten, M., de Pater, S., Romeijn, R., van Schendel, R., Hooykaas, P. J. J., & Tijsterman, M. (2016). T-DNA integration in plants results from polymerase-θ-mediated DNA repair. *Nature plants*, 2, 16164.
Winans, S. C. (1992). Two-way chemical signaling in *Agrobacterium*-plant interactions. *Microbiological reviews*, 56, 12-31.
Ward, E. R., & Barnes, W. M. (1988). VirD2 protein of *Agrobacterium tumefaciens* very tightly linked to the 5'end of T-strand DNA. *Science*, 242, 927.
Yadav, N. S., Vanderleyden, J., Bennett, D. R., Barnes, W. M., & Chilton, M. D. (1982). Short direct repeats flank the T-DNA on a nopaline Ti plasmid. *Proceedings of the National Academy of Sciences*, 79, 6322-6326.
Zhang, X., van Heusden, G. P. H., & Hooykaas, P. J. J. (2017). Virulence protein VirD5 of *Agrobacterium tumefaciens* binds to kinetochores in host cells via an interaction with Spt4. *Proceedings of the National Academy of Sciences*, 114, 10238-10243.
Zhu, J., Oger, P. M., Schrammeijer, B., Hooykaas, P. J.J., Farrand, S. K., & Winans, S. C. (2000). The bases of crown gall tumorigenesis. *Journal of Bacteriology*, 182, 3885-3895.